The Pennsylvania State University

The Graduate School

LIGHT AVAILABILITY ALONG DEPTH GRADIENTS: A KEY DRIVER OF NICHE PARTITIONING AND BIODIVERSITY PATTERNS IN REEF BUILDING CORALS

A Dissertation in

Biology

by

Tomás López-Londoño

Submitted in Partial Fulfillment
of the Requirements
for the Degree of

Doctor of Philosophy

May 2022

The dissertation of Tomás López-Londoño was reviewed and approved by the following:

Roberto Iglesias-Prieto
Professor of Biology
Dissertation Advisor

Mónica Medina
Professor of Biology
Chair of Committee

Todd C. LaJeunesse
Professor of Biology

Jonathan Lynch
Distinguished Professor of Plant Nutrition

Elizabeth A. McGraw
Professor and Department Head of Biology

ABSTRACT

The ecological success of corals in oligotrophic tropical environments since the Late Triassic is attributed to the nutritional advantages derived from the symbiosis with photosynthesizing dinoflagellates[1] and their extraordinary efficiency in collecting and using solar energy for carbon fixation[2]. The energetic gains conferred by the photosymbiosis significantly enhances coral calcification[3,4] which, ultimately, enabled the consolidation of one of the most biodiverse ecosystems on the planet: coral reefs[5]. Due to the sunlight dependence to power metabolism, symbiotic corals are restricted to the photic zone of the world's oceans where light is enough to allow photosynthesis[6]. Importantly, because of the exponential extinction of light with depth, their vertical distribution in the photic zone occurs along steep gradients of irradiance in typically small spatial scales, such as dozens of meters, while other limiting resources and physical factors remain relatively constant[7,8]. These traits, together with the great dispersal potential associated with a planktonic larval stage in the life cycle, make scleractinian corals a particularly interesting taxa to explore the effects of light availability on global patterns of biodiversity and the spatial organization of ecological communities, while avoiding potential confounding factors such as scale-dependent effects and dispersal boundaries of species[9].

The optical properties of the water column, correlated with the vertical attenuation coefficient for downwelling irradiance (K_d)[6], determine to a great extent the characteristics of the underwater light field and the depth of the photic zone. For example, the lower limit of the photic zone in turbid-waters with high K_d (*e.g.,* Varadero with K_d of 0.193 m^{-2} [10]) is estimated to be nearly 20 m, while in clear-waters with low K_d (*e.g.,* the Red Sea with K_d of 0.047 m^{-2} [11]) it can be almost 100 m. Moreover, the spectral composition of the underwater light field also changes according to the local K_d, typically because a wavelength-selective absorption towards the blue end of the spectrum in waters with high K_d[10,12]. This illustrates the importance of considering the local optical properties of the water column not only for determining the maximum depth that can sustain symbiotic corals, but also for exploring the association between depth, local light climate, photoacclimation status, and structure of symbiotic coral communities.

The *Orbicella* spp. complex is a major reef builder in the Caribbean exhibiting a vertical distribution that spans the entire photic zone[13,14]. This species complex was originally regarded as one species with ecotypic variation, but recent research revealed the existence of three species

partially segregated by depth[15,16]. *O. annularis* (Ellis and Solander, 1786) forms disjunct columns with senescent edges, being consistently found in shallow-waters between 1 m and ~20 m. *O. franksi* (Gregory, 1895) forms irregular mounds and plates and is typically found deeper than its two sibling species (up to depths of 60 m). *O. faveolata* (Ellis and Solander, 1786) forms massive mounds and can partially overlap with both *O. annularis* and *O. franksi* habitats[13,14]. The symbiotic dinoflagellate communities[17-19] and the photobiology of this species complex have been extensively studied[20-22], enabling the identification of important differences determined by light availability within colonies and across depths. Therefore, these recently diverged coral species offer an ideal system to study how corals specialize to live in different habitats across depth-mediated light gradients and the importance of niche specialization for the maintenance of corals diversity.

In my dissertation, I have studied the effects of the physical interaction between light, the water column and corals at multiple levels of biological organization, from individuals and populations to reef coral communities. I considered physical and physiological principles that govern the vertical distribution of light in the water column and the photosynthetic activity of primary producers, including the symbiotic algae of corals. Some of my research has been focused on *Orbicella* spp. because of the ecological, morphological and physiological traits that characterize this species complex. In the first chapter, I tested the predictions of the species-energy hypothesis for explaining biodiversity patterns in symbiotic coral communities across depth gradients. In the second chapter, I explored the physiological and ecological consequences of the water optical properties degradation associated with anthropogenic pollution on reef corals. And lastly, in the third chapter, I studied the physiological strategies and photoacclimation potential leading to niche partitioning driven by light gradients in sibling species of corals.

TABLE OF CONTENTS

LIST OF FIGURES

LIST OF TABLES

ACKNOWLEDGEMENTS

I want to thank my family and my partner, Mitzy Porras, for your patience and for being an invaluable source of inspiration and support in this endeavor.

I want to express my deepest gratitude to my advisor, Roberto Iglesias-Prieto, for your patience, support, enthusiasm and guidance over the last years. I also wish to acknowledge my appreciation to my committee members Mónica Medina, Todd LaJeunesse and Jonathan Lynch for providing insight and guidance. I feel very fortunate to have met you and had the chance to work with you.

I also want to thank my lab mates, both past and present, especially to Claudia Tatiana 'Tati' Galindo, Luis González, Kelly Gómez, Naomi Huntley, and Darren Brown, for your continued support and feedback. I would also like to thank to current and past members of the Medina Lab, LaJeunesse Lab and Baums Lab for your accessibility and willingness to share your insights and wisdom.

Lastly, I want to thank my funding sources, including the Pennsylvania State University startup funds to Roberto Iglesias-Prieto and Mónica Medina; Pennsylvania State University SSRI and IEE grants; National Science Foundation (NSF) under grants OCE 1442206, OCE 1642311 and OIA 2032919; and National Oceanic and Atmospheric Administration (NOAA) under grant NA19NOS4820132. Any opinions, findings, and conclusions or recommendations expressed in this publication are those of my coauthors and myself and do not necessarily reflect the views of any of these funding sources.

PREFACE

My contribution to the multi-authored work included in each one of the following chapters was substantial, and each manuscript was integral to my dissertation. For all these manuscripts, I participated in the research conceptualization, experimental design, field work (when a field component was part of the research), data collection, data analysis (modelling, environmental conditions, hydrologic optics and physiology), and writing.

In the manuscript submitted as part of the Chapter 1, I substantially participated in the research conceptualization, methodology, investigation, meta-analysis, modelling, data visualization, and writing. In the manuscript submitted as part of the Chapter 2, I substantially participated in the experimental design, field work, data collection, analysis of water optics and environmental conditions, physiological and ecological analysis, data visualization, and writing. In the manuscript submitted as part of the Chapter 3, I substantially participated in the field work, data collection, analysis of water optics and environmental conditions, physiological analysis, manuscript conceptualization, data visualization, and writing. In this last manuscript, I'm sharing the first authorship with Dr. Carlos Prada.

Chapter 1

Photosynthetic energy supply drives biodiversity patterns in reef corals

Manuscript submitted to *Science Advances*

Authors

Tomás López-Londoño[1]*, Kelly Gómez-Campo[1], Xavier Hernández-Pech[2], Susana Enríquez[2], Roberto Iglesias-Prieto[1]*

Affiliations

[1]*Pennsylvania State University, Department of Biology; University Park, PA 16802, USA.*

[2]*Unidad Académica de Sistemas Arrecifales, Instituto de Ciencias del Mar y Limnología, Universidad Nacional Autónoma de México; Cancún, Quintana Roo 77500, México.*

**Corresponding authors*

Abstract

Coral reefs are hyperdiverse ecosystems, yet their biodiversity is heterogeneously distributed over space and time following patterns commonly attributed to biogeographic factors and disturbance regimes[23-25]. Contrary to terrestrial environments[26], the amount of usable energy, or primary productivity, has received little attention and empirical support[9] for explaining such patterns[27]. Possible reasons for this discrepancy are the surrogates used as roughly indicative of productivity and the confounding effect of environmental stressors[28,29], typically more accentuated in high-productivity portions of reefs (*e.g.*, shallow-water)[11]. Here we explore the productivity-biodiversity relationship in symbiotic corals -the foundation species of these ecosystems- from reefs with contrasting geological history and environmental conditions, encompassing the major hotspots of coral biodiversity. We use a relatively simple, but physiologically robust, mechanistic model to simulate the depth-dependent variation of the photosynthetically derived energy supplied by the symbiotic algae to their coral hosts. The model incorporates light availability mediated by local attenuation coefficients, algal primary productivity and the costs associated with the repair of the photosynthetic apparatus, following optical[6] and physiological principles[30]

as well as empirical evidence. Our model significantly explains between 60 and 97% variation of coral biodiversity across depths for all reefs tested, suggesting that changes in coral biodiversity across depths are primarily driven not by changes in species composition or local deterministic factors but by changes in the fractional contribution of photosynthetically derived energy by the symbiotic algae to their hosts. Our findings highlight the fundamental role of the photosymbiosis in reef-building corals at the most complex levels of ecological organization, urging action to preserve the water optical quality to counterbalance the biodiversity erosion in coral reef communities.

Introduction

One of the underlying premises of macroecology is that much of the variation in ecological communities assembly is driven by a few predictable, deterministic processes that can be quantitatively described[31,32]. Among the different processes that have been correlated with species diversity is habitat productivity[28,29]. A mechanistic explanation for this relationship is provided by the species-energy hypothesis (SEH)[27], which proposes that the supply of usable energy plays a decisive role in the determination of species diversity. According to the SEH, if increased productivity leads to increased population densities, the result would be increased biodiversity because of decreased risk of species extinction from demographic and environmental stochasticity. However, significant debate remains over the strength of this linkage and whether it is predictable, especially so considering the important variation in forms of the productivity-biodiversity relationship (*e.g.*, positive, negative, unimodal and neutral) and our incomplete understanding of the causes of such variation[33-36], which have made it difficult to reach a general consensus on whether productivity is a universal process driving the spatial organization of biodiversity. Since the amount of usable energy by a group of organisms is difficult to measure directly, part of this variation may be associated with the surrogates used as roughly indicative of productivity and the confounding effects of environmental stressors, typically more accentuated in highly productive environments[28,29].

Scleractinian corals are responsible for building one of the most diverse and productive ecosystems on Earth. Their ecological success in oligotrophic tropical environments since the Late Triassic is attributed to the nutritional symbiosis with photosynthesizing dinoflagellates (also known as zooxanthellae)[37] and their extraordinary efficiency in collecting and using solar energy for carbon fixation[2]. Due to the exponential attenuation of light with depth[6], the vertical

distribution of symbiotic coral species occurs along step gradients of irradiance in typically small spatial scales such as dozens of meters while other limiting resources and physical factors (*e.g.*, nitrogen, oxygen, temperature) remain relatively constant[7,8]. These traits, together with the great dispersal potential associated with a larval stage in the life cycle, make scleractinian coral communities particularly interesting to explore the biodiversity-productivity relationship while avoiding confounding factors such as scale-dependent effects and dispersal boundaries of species. Nevertheless, the productivity-biodiversity relationship has received little support in coral communities research[9], where historic and biogeographic factors as well as disturbance regimes have been identified as the most common factors associated with the spatial variation of diversity[23-25] (but see [26]).

To explore the productivity-biodiversity relationship in coral communities, it is important to note that sunlight not only represents an essential energetic resource for growth and survivorship, but also a potential physiological challenge for coral holobionts when the light energy absorbed exceeds that required for algal photosynthesis[38,39]. This energetic imbalance results from the linear relationship between light availability and light absorption on the one side and the hyperbolic response of photosynthesis to light availability on the other, which ultimately leads to a disparity between the cost to maintain the photosynthetic activity and the chemical energy derived from photosynthesis[30]. Photoprotection and repair of the photosynthetic apparatus are two fundamental processes to compensate this energetic imbalance and maintain an optimal photosynthetic activity in particular light and temperature regimes[30,38]. Although these processes have been intensively studied on corals and their algal symbionts during last decades[40,41], their implications on the energetic performance of coral holobionts at the community and ecological levels have been largely neglected.

The physiological basis of the coral-algae symbiosis and the predictable behavior of light across depth gradients make coral communities ideal systems to test the predictions of the SEH. Here, using a mechanistic model based on underwater optics and physiological principles, we tested whether the photosynthetically derived energy available to corals can explain patterns of coral species diversity across depths. We tested the model using published datasets from reefs with contrasting evolutionary histories, environmental conditions, and the most common distribution patterns of coral richness, encompassing the three centers of coral diversity of the world's major ocean basins.

Materials and Methods

Estimation of the symbiotic algae variable energy budget

We assume that the energy expenditure in photorepair by the symbiotic algae (C_s) is mediated by the light exposure (*i.e.*, photosynthetic activity), limiting the photosynthetic energy supply to coral hosts (*PES*) across depths. In this analysis, *PES* is correlative with the "contribution of carbon from zooxanthellae to coral animal respiration" or CZAR, a concept originally introduced by Muscatine et al.[42]. In their original formulation, however, the translocation of photosynthetically fixed carbon was calculated based on the oxygen production/consumption of the holobiont using a conversion factor that was independent of light availability.

We estimated the pattern of change of C_s as a function of light exposure in small fragments (~5x5 cm, n=50) of the Caribbean coral *Porites astreoides* collected from La Bocana Reef at 5 m depth in Puerto Morelos, México. Corals were initially acclimated to laboratory conditions in a running seawater aquarium with neutral density filters simulating the light intensity at the collection site. Two weeks after acclimation to laboratory conditions, corals were exposed to contrasting light intensities to measure changes in: 1) the photosystem II (PSII) photochemical quantum yield ($\Delta F/F_m$') over diurnal cycles using the pulse amplitude modulated (PAM) technique[43], and 2) the PSII half-time by analyzing the diurnal oscillation of $\Delta F/F_m$' of coral fragments exposed to 100 µg of chloramphenicol (CAP), a chloroplast protein-synthesis inhibitor[44]. The PSII $t_{1/2}$ was calculated as the amount of time required to inactivate 50% of the PSII. While this analysis was conducted using only one coral species, the overall change of $\Delta F/F_m$' and PSII $t_{1/2}$ as a function of irradiance is expected to follow similar patterns in different coral-algae associations due to the direct relationship between light exposure and the dynamic photoinactivation and repair of PSII reaction centers in symbiotic dinoflagellates[45-47] (Figure **1-1A**).

We used the following equation to calculate the PSII $t_{1/2}$ (in h) as a function of available irradiance:

$$\text{PSII } t_{1/2} = M\, E_{z\%}^{\Delta}, \qquad \text{(Equation 1-1)}$$

where M is the maximum PSII half-time when the available irradiance tends to 0, and Δ is the rate of change of PSII half-time with respect to the available irradiance.

We estimated the energy expenditure in photorepair by the symbiotic algae (C_s) in 12 hours cycles of light-induced photosynthetic activity through the following relation:

$$C_s = (12 / \text{PSII } t_{1/2})\ R, \qquad \text{(Equation 1-2)}$$

where R is the relative energy costs of PSII reaction centers turnover in the photosynthetic apparatus of the symbiotic algae.

Description of the coral productivity-biodiversity model

To estimate photosynthetic energy supply (*PES*) by the symbiotic algae to corals across depth gradients we used a numerical model with a lumped-parameter approach acknowledging three physical and physiological principles that govern the vertical distribution of light in the water column and the photosynthetic activity of primary producers. These principles are: 1) Solar radiation diminishes exponentially with depth according to the optical properties of the water column (*i.e.*, local K_d); 2) Algal photosynthetic production describes a non-rectangular hyperbolic response to light availability; and 3) Energy expenditure in repair the photodamaged photosynthetic apparatus of the symbiotic algae is mediated by the light exposure following *equation 1*. The model assumes that a specific set of parameters represents the average response of the coral community[48]. This approach allows to draw general conclusions about light-driven processes at the community level at the expense of simplifying the complex dynamics of the water optical properties[49,50], and acclimation strategies of corals to maximize performance under particular light and temperature regimes[51-53].

The available irradiance across depths, as the energy source for the symbiotic algae to fix inorganic carbon via photosynthesis, is calculated in accordance to Kirk[6] as:

$$E_z = E_0\ e^{-K_d z} \qquad \text{(Equation 1-3)},$$

where E_z and E_0 are the irradiance (E) at depth z and just below the sea surface, respectively.

The hyperbolic response of algal photosynthesis (P_g) to irradiance is calculated according to Jassby and Platt [54], as:

$$P_g = P_{max} \tanh (\alpha\ E_z / P_{max}) \qquad \text{(Equation 1-4)},$$

where α is the photosynthetic efficiency corresponding to the slope of the linear increase of photosynthesis at subsaturating irradiance and P_{max} is the maximum photosynthetic rates at light

saturation. We assume no temporal reduction in light-saturated photosynthesis in response to photoinhibition at excessive irradiance considering the apparent absence of this phenomenon in symbiotic dinoflagellates *in hospite*[45].

Finally, the photosynthetic energy supply (*PES*) for the coral is parameterized with the following equation:

$$PES = P_g - C_s \qquad \text{(Equation 1-5)}.$$

Testing the productivity-biodiversity model against empirical data

To test the capacity of the productivity-biodiversity model to explain coral species richness variation with depth, we analyzed published datasets from studies conducted in a wide range of reefs with contrasting geological history and environmental conditions, encompassing the three major hotspots of coral biodiversity[55,56]. These studies reported the change in number of symbiotic coral species across depths, covering the main biodiversity patterns (unimodal, monotonic increase and monotonic decrease)[9,57-60]. Data were extracted directly from the text, tables, or original datasets. When the data was only presented in graphical format, raw values were extracted by using the WebPlotDigitizer version 4.4 (https://automeris.io/WebPlotDigitizer). When the local K_d was not reported in the manuscript, it was calculated from the light change across depths following *equation 2*. When neither of these options was available, it was extracted from the literature for the same or a comparable site.

For each site, a two-step optimization procedure was used to calculate those parameters that could not be estimated independently with empirical data. The optimization of these parameters produced the best possible fit between the model output and the mean number of observed species across depths. First, an iterative algorithm that allow the variation of each parameter within a suspected range while fulfilling the model equations exactly, was used for fitting a linear model with coral richness as a function of the available energy across depths. Using the Akaike Information Criterion (AIC), we selected the set of values that minimized the misfit between the productivity-biodiversity model output and the empirical data. Then, the values of the targeted parameters that minimized the AIC were used as the starting values in a bound-constrained minimization algorithm (*optim* function) based on the Nelder-Mead method[61]. The lower and upper bounds of each parameter were determined based on empiric data and physiological limits and were constant among sites. A diurnal cycle of solar radiation describing a 12h sinusoidal

curve peaking at 1,800 μmol quanta m^{-2} s^{-1} at noon was used as forcing function (chosen maximum is a random value close to naturally occurring maximum irradiance at ocean surface in tropical areas[6]). An Analysis of Covariance (ANCOVA) was conducted to test for differences in the slope of the model across sites (*i.e.*, rate of change in the number of species with the amount of available energy to coral hosts). All analyses were conducted using R version 3.6.1[62].

Results

Estimation of the symbiotic algae variable energy budget

To measure the light-dependent kinetics of the photosystem II (PSII) damage and repair cycle, we measured the effective quantum yield of PSII ($\Delta F/F_m$') over diurnal cycles in the coral *Porites astreoides* using pulse amplitude modulated (PAM) fluorometry. This analysis indicated that the pattern of change of $\Delta F/F_m$' followed an inverse relationship with light availability; decreasing after dawn to reach minimum values around midday and then gradually recovering by dusk[63-65]. The maximum reduction of $\Delta F/F_m$' at noon and its recovery by late afternoon were not constant between days, showing an incomplete recovery when the light exposure was increased (+50% relative to photoacclimation) and full recovery exceeding former dawn levels when the light exposure was reduced (-50%) (Figure **1-1A**). The fluctuation of the effective quantum yield of PSII reflected differences in the accumulation of photodamaged reaction centers in response to the total light exposure[45,46].

To complement this analysis, we measured changes in the PSII half-time ($t_{1/2}$) as a function of irradiance using the chloroplast protein synthesis inhibitor "chloramphenicol". The relationship of PSII $t_{1/2}$ to light exposure was described by a two-parameter power function fitted by standard non-linear regression ($r^2 = 0.97$, $p < 0.01$). This function indicated that the PSII $t_{1/2}$ in the photosynthetic apparatus of symbiotic dinoflagellates of *P. astreoides* is proportional to the available irradiance (% sea surface) following a scaling relationship (**Figure 1-1B**). Experiments conducted with other coral species (*Orbicella faveolata*) have yielded very similar results (Gómez-Campo, unpublished data), suggesting that the observed pattern of change in PSII $t_{1/2}$ as a function of irradiance may be generalized among symbiotic dinoflagellates of reef corals.

The variation of $\Delta F/F_m$' and PSII $t_{1/2}$ indicated that the energetic cost of repair photodamaged PSII reaction centers for optimizing the algal photosynthetic performance is mediated by light

exposure. A conceptual analysis of the changes in the maximum excitation pressure over PSII (Q_m) as a function of irradiance suggests that both the shortage and excess of light can compromise the energetic performance of the coral holobiont (Figure **1-1C**). This compromise results from a negligible photosynthetic activity and energetic contribution of the symbiotic algae under light-limiting conditions and full saturation of the photosynthetic apparatus associated with increased costs of repair from photodamage under excessive irradiance[20,43].

The functional relationship between light availability, gross productivity (P_g) and energy expenditure in photorepair by the symbiotic algae (C_s), generates a hump-shaped curve of the energy available to corals with depth (Figure **1-1D**). The shape of the curve is explained by two opposite processes that lead to a reduction in photosynthetic energy supply (*PES*) to corals at both ends of the depth-mediated light gradient: 1) in shallow high-light environments, where irradiance normally exceeds the light saturation point for photosynthesis (E_k) during most of the day[66], the maintenance costs of the algal photosynthetic activity are significantly enhanced while photosynthesis is fully saturated (*i.e.,* there is no increase in carbon fixation); and 2) in deep low-light environments, the attenuation of light with depth results in a gradual decline of the photosynthetically fixed energy by the symbiotic algae.

Testing the productivity-biodiversity model against empirical data

The productivity-biodiversity model accurately explained the variation in species number across depths in all reef habitats despite local differences in reef geological history, environmental conditions, and level of diversity (Figure **1-2**). The variation in coral species richness explained by *PES* fluctuated between 64% and 95%, being lower at those sites with an apparently incomplete sampling of the coral community (*i.e.,* positive and negative monotonic relationships reported in the Red Sea[58] and Singapore[60], respectively) (Figure **1-2, Appendix**). However, even at these sites, the model captured the general pattern of change in species richness and the number of observed species did not differ significantly from those predicted by the model. The slope of the model was significantly different across locations ($F_{(6,50)} = 35.44$, $p < 0.001$) indicating that, although the relationship between photosynthetic energy availability and coral species richness was constant, the rate of change in species number as a function of energy availability varied significantly between sites (**Appendix**).

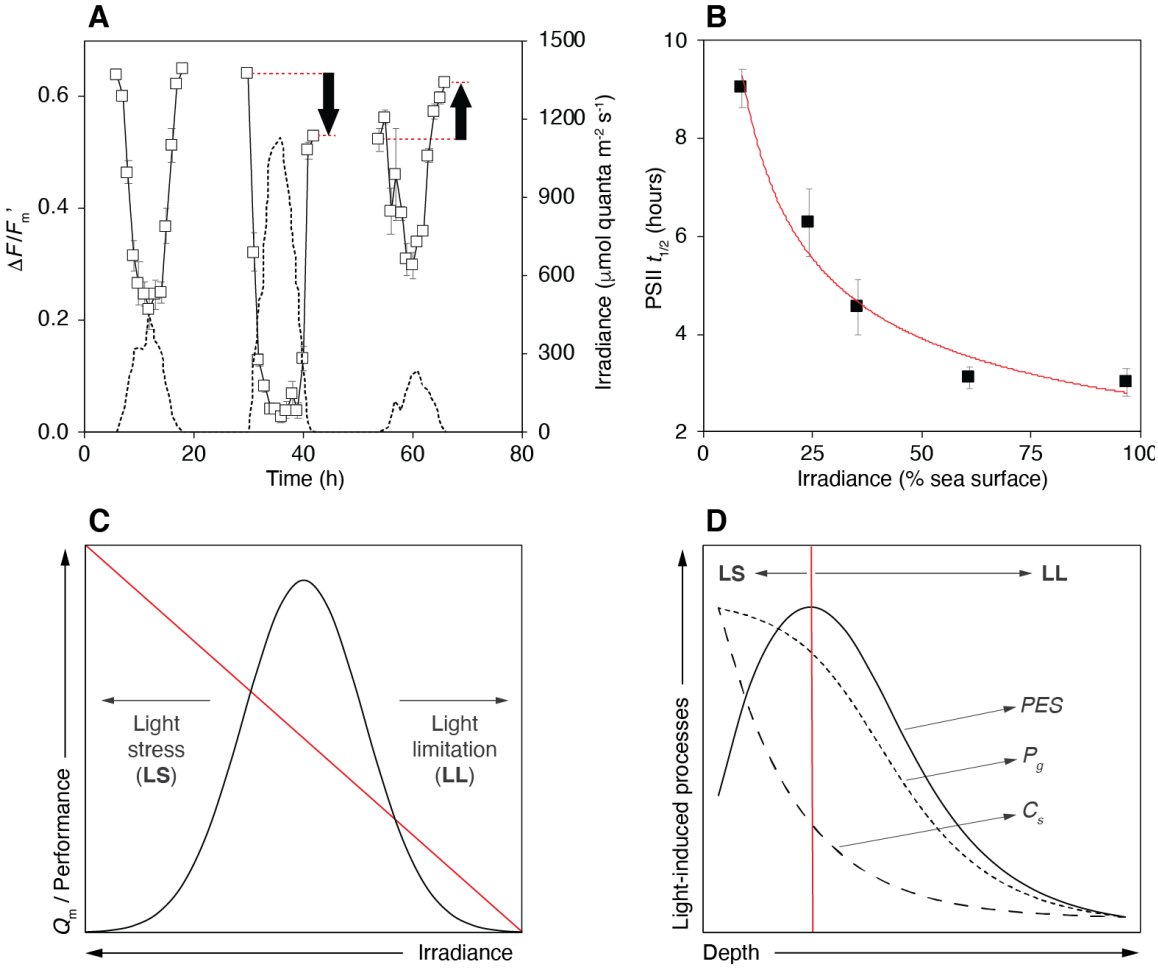

Figure **1-1**: Principles and components of the productivity-biodiversity model. **A** Diurnal variation of $\Delta F/F_m$' in symbionts of *Porites astreoides* measured experimentally during a control-reference day (first day), and during days with increased (second day) and reduced irradiance (third day). Broken lines represent diurnal changes in irradiance. **B** Changes in the PSII $t_{1/2}$ in response to contrasting light exposure (% of sea surface irradiance). **C** Theoretical behavior of coral holobiont energetic performance (black line) in relation to Q_m (red line) across a depth-mediated light gradient, highlighting the predicted effects of light stress (LS) and light limitation (LL) on coral holobionts performance. **D** Schematic representation of the relative changes in light-induced processes affecting the energy balance of the coral-algal symbiosis across a depth gradient: photosynthetic energy available to corals (continuous line), C_s (long dashes), and P_g (short dashes). The theoretical turning point between increasing light stress and light limitation is indicated with a red vertical line.

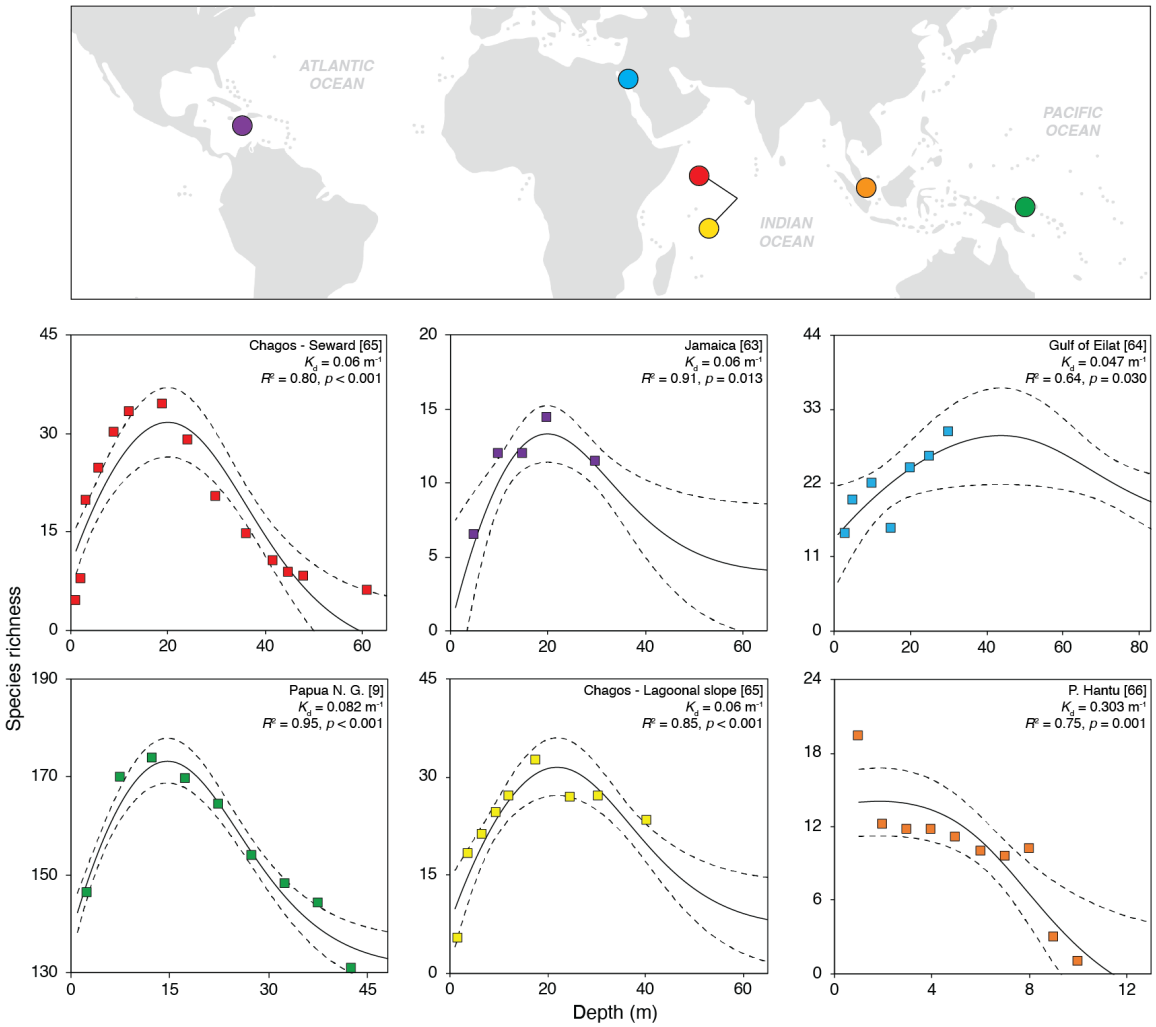

Figure **1-2**: Coral species richness variation along depth gradients in reefs across the world's major centers of biodiversity. The observed distribution of species diversity (squares) is significantly explained by the productivity-biodiversity model at all sites. Continuous lines represent the trend in mean values and the discontinuous lines 95% confidence intervals. It is indicated the goodness-of-fit (R^2) and the statistical significance of the model (p-value) at each site, together with the local K_d. Species richness were projected to depths at which the light intensity was estimated to be 2% of sea surface.

We projected the species richness distribution within sites into a global light intensity gradient mediated by the vertical attenuation coefficients for downwelling irradiance (K_d's), which were extracted from the literature (**Appendix A**). This analysis corroborated that the change in species richness across the light intensity gradient is not random but follows a unimodal, bell-shaped pattern with an overall reduction in the relative number of species at both ends of the gradient (Figure **1-3**), consistent with biodiversity patterns in other photosymbiotic anthozoans like

octocorals[67]. This may explain why previous studies haven't found a significant linear relationship between species richness and energy when using solar radiation as the proxy of energy available for the coral community[9]. The bell-shaped relationship between species richness and light availability is consistent with the predictions of the coral holobionts energetic performance across the light gradient (Figure **1-1C**).

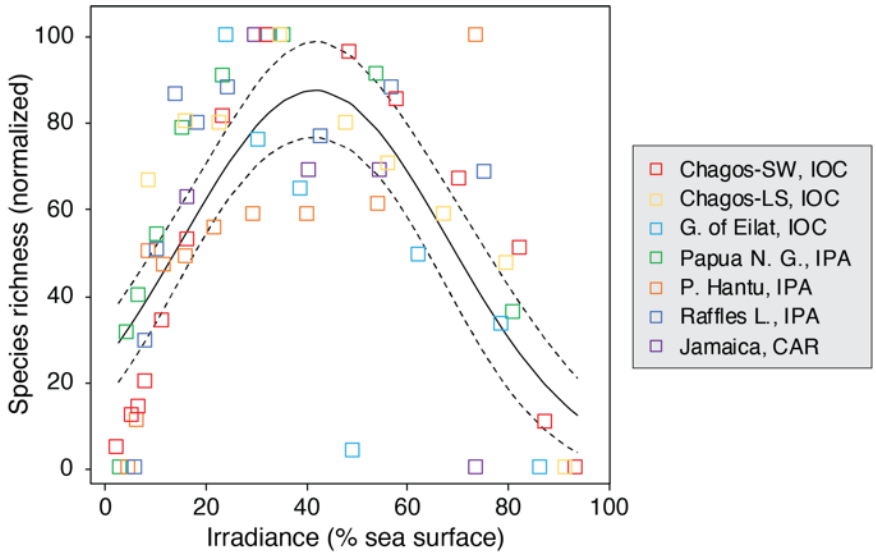

Figure **1-3**: Variation in species richness across an irradiance gradient (in % relative to sea surface) mediated by the optical properties of the water column (K_d) at each site. The overall data was fitted using a gaussian function (continuous line) with 95% confidence intervals (discontinuous lines).

Discussion

The results of this work suggest that changes in coral biodiversity across depth gradients are primarily driven not by changes in species composition or local deterministic factors but by changes in the fractional contribution of photosynthetically derived energy by the symbiotic algae to their hosts. These findings are consistent with the predictions of the species-energy hypothesis (SEH), highlighting the fundamental role of light-induced processes, including algal primary production and energy expenditure, in the spatial organization of coral communities. The lack of prior support for the SEH in coral communities[9] may result from unclear definitions of the actual energy physiologically available to the coral animal (*e.g.*, solar energy). This contradiction

illustrates the persistent difficulty of actually measuring the energy available to organisms in studies of species richness-productivity relationships and choosing the energy-related variable that best predicts richness variation according to the system studied[27-29].

Our analysis indicates that coral richness follows a linear relationship with the photosynthetic energy availability for corals (*i.e.*, there is a monotonic increase in diversity with the energy translocated by the symbiotic algae). However, the productivity-biodiversity relationship results in a hump-shaped pattern across depth gradients due to the non-linearity between depth, light availability, and the symbiotic algae photosynthetic activity and energy expenditure. The increasing and decreasing phases of the humpback species-richness curve across depth gradients seem to result from two contrasting conditions that limit the energetic output of the symbiotic algae and the coral holobiont performance. In low-light environments (the increasing phase of the richness curve), which can occur in a wide range of depths depending on the local K_d, the deprivation of light-energy results in a deficit of photosynthetically fixed carbon that can be translocated to the coral animal. Whereas in high-light environments (the decreasing phase of the curve), typically shallow waters, the increased costs of repair the algal photosynthetic apparatus while photosynthesis is fully saturated limits the amount of energy that can be translocated to their coral host. This condition is coupled with a strong selective pressure exerted by intense light, including high UVR[68,69]. Toward both ends of the light intensity gradient, the reduced photosynthetic energy availability may lead to an increased risk of extinction of coral species[27] and prevalence of few efficient competitors at exploiting the available light energy, either in excess or deficit. At intermediate irradiance, close to the light-saturation point of photosynthesis (E_k), the energetic output of the symbiotic algae and the coral holobiont performance are expected to reach their maximum potential. The depth range in which this optimum irradiance occurs will have the lowest rate of species extinction and highest coral biodiversity, according to the SEH predictions[27].

Particular colony morphologies that allow the coral animal to regulate light capture[51,70] and associations with species of symbionts with contrasting photoacclimative capabilities[17,43], which collectively determine the light niche of coral species[43,71], will be selected along the depth-mediated light gradient. It may be that the combinations between colony morphologies and species-specific associations with algal symbionts are potentially higher within a range close to the optimum irradiance. The larger energy supply of the symbiotic algae may lead to increased coral biodiversity because of decreased risk of species extinction, according to the SEH. But also,

the increased energy availability may promote a more widely available specialization (*i.e.,* niche) space and evolutionary innovation with regard to colony geometry, skeleton morphology and symbiont associations, allowing more species to coexist in the coral community[33]. Conversely, the variety of viable specializations that emerge from combinations between colony morphology and algal associations are predicted to be lower at both ends of the light intensity gradient due to reduced resource heterogeneity[28].

Environmental conditions contributing to variation in biodiversity patterns

Environmental stressors whose effects are more pronounced in shallow-waters can blur the association between photosynthetic energy availability and coral species richness across depths. There are two potentially major sources of stress in shallow waters that have little impact toward deep habitats: coral bleaching events, which often lead to widespread coral mortality, and physical disturbance associated with storms and hurricanes[8,11]. Coral bleaching (*i.e.*, the disruption of the symbiotic relationship with endozoic algae) results from the synergistic effect of temperature and light intensity on the holobiont photosynthetic performance[72,73]. Recent studies have shown that moderate reductions in light availability associated with water turbidity can reduce bleaching impacts in shallow-water reef environments[74-76], which have led to hypothesize that turbid reefs may serve as climate-change refuge for corals. Our results suggest that, although some level of water turbidity may protect shallow-water corals from thermal stress, the hypothesis that turbid reefs may serve as climate-change refuge for corals should be cautiously considered due to, on the one hand, the reduced coral diversity that is being protected corresponding to the increasing phase of the unimodal richness curve and, on the other, the occurrence of genetically differentiated ecotypes within and between species segregated by local ecological factors[77,78], which may not be able to survive in high-light environments.

In addition, storms and hurricanes have obvious effects on ecological communities and it has been hypothesized that an intermediate exposure to disturbances may determine greater biodiversity[23]. The intermediate disturbance hypothesis, originally proposed as a conceptual model, has been supported and rejected in its capacity for explaining biodiversity patterns in ecological communities (reviewed by Rosenzweig and Abramsky[28] and Huston[35]). Certainly, disturbances influence both the local species diversity and the community structure of symbiotic corals. However, the consistency of the productivity-biodiversity model despite local environmental and ecological conditions among sites indicates that disturbances and other

environmental factors may alter the location of the mode as well as the slope of the increasing and/or decreasing phase of the unimodal curve, but not the overall pattern of corals' diversity with depth. Thus, our results indicate that analyzing the effects of disturbances on biodiversity ignoring the role of the photosynthetic energy availability for corals can obscure the underlying cause of biodiversity patterns in coral communities.

Another aspect that may affect the energy budget of symbiotic coral species is heterotrophy[79-81]. Given their mixotrophic nature, at least some coral species are able to increase their metabolic reliance on heterotrophy to compensate for reduced photosynthetically derived energy acquisition in low-light environments (reviewed by Houlbrèque and Ferrier-Pagès[82]). We did not parameterize this aspect of the symbiosis in the productivity-biodiversity model and cannot discharge a potential effect of heterotrophic plasticity on coral richness. However, the contrasting features exhibited by zooxanthellate (non-facultative) corals in low-light environments suggest adaptation and specialization to maximize light capture, more than increasing heterotrophic feeding capabilities [11]. For instance, if heterotrophy played a significant role in extending the vertical distribution of symbiotic corals, a greater number of species with morphologies that facilitate suspension feeding (*e.g.*, branching) will be expected to thrive with increasing depth. However, the empirical evidence indicates that flattened morphologies to maximize light capture prevail in the lower photic zone[11,83].

Our results indicate that although solar energy is not the only source of energy for symbiotic corals, it may be one of the major driving forces of biodiversity patterns in reef coral communities. The symbiosis with photosynthesizing dinoflagellates was a successful adaptive solution for corals to thrive in oligotrophic environments[37] which, ultimately, led to the consolidation of one of the most biodiverse ecosystems on the planet. The gradient of downwelling irradiance mediated by the water optical properties coupled with the metabolic, physiological and morphological constraints imposed by the photosymbiosis are the primary ingredients for the establishment of global-scale patterns of biodiversity in scleractinian corals and, potentially, other symbiotic anthozoans[67]. The increased degradation of the water optical quality associated with coastal development, nutrient enrichment, and terrestrial runoff to which most of the world's reefs are currently exposed[84,85], may be an important underling cause of biodiversity erosion and change in the assemblage structure of coral reef communities. Local conservation actions seeking to preserve the water optical quality and the underwater light

climate are essential to preserve coral biodiversity while concerted global action to limit greenhouse emissions and slow global warming continue to move forward.

Chapter 2

Physiological and ecological consequences of the water optical properties degradation on reef corals

Manuscript published in *Coral Reefs 40:1243–1256*

https://doi.org/10.1007/s00338-021-02133-7

Authors

Tomás López-Londoño,[1]* Claudia T. Galindo-Martínez,[1] Kelly Gómez-Campo,[1] Luis A. González-Guerrero,[1] Sofia Roitman,[1] F. Joseph Pollock,[1] Valeria Pizarro,[2] Mateo López-Victoria,[3] Mónica Medina,[1] Roberto Iglesias-Prieto[1]*

Affiliations

[1]*The Pennsylvania State University, Department of Biology; University Park, PA 16802, USA.*

[2]*The Nature Conservancy, The Cape Eleuthera Island School, Rock Sound, Bahamas*

[3]*Pontificia Universidad Javeriana, Department of Natural Sciences and Mathematics, Cali, Colombia*

**Corresponding authors*

Abstract

Degradation of water optical properties due to anthropogenic disturbances is a common phenomenon in coastal waters globally. Although this condition is associated with multiple drivers that affect corals health in multiple ways, its effect on light availability and photosynthetic energy acquisition has been largely neglected. Here, we describe how declining the water optical quality in a coastal reef exposed to a turbid plume of water originating from a man-made channel compromises the functionality of the keystone coral species *Orbicella faveolata*. We found highly variable water optical conditions with significant effects on the light quantity and quality available for corals. Low-light phenotypes close to theoretical limits of photoacclimation were found at shallow depths as a result of reduced light penetration. The estimated photosynthetically fixed energy depletion with increasing depth was associated with patterns of colony mortality and vertical habitat compression. A numerical model illustrates the potential effect of the progressive

water quality degradation on coral mortality and population decline along the depth gradient. Collectively, our findings suggest that preserving the water properties seeking to maximize light penetration through the water column is essential for maintaining the coral reef structure and associated ecosystem services.

Introduction

Coral reefs are recognized not only as one of the most complex, productive and biologically diverse ecosystems[86], but also as icons of the devastating effects of anthropogenic stressors to the natural environment. We have already lost nearly a quarter of the world's coral reefs, with the largest cause being the increasing frequency and magnitude of massive climate-related bleaching events[87,88]. Reefs in the Indo-Pacific and the Caribbean, in particular, have lost nearly half of their coral cover due to human impacts[89,90]. Approximately 75% of remaining reef areas are rated as threatened due to the synergistic effects of large-scale stressors and regional and local factors such as water pollution and overfishing[85,91-93].

Ample evidence demonstrates that water-quality deterioration affects reef corals in different ways. Two main stress-related factors are: a) interference of nutrient enrichment in the host's capacity to control populations of algal symbionts and opportunistic microorganisms (*e.g.,* Symbiodiniaceae and bacteria)[94,95]; and b) disease prevalence and energetic losses resulting from the physical disturbance of particle abrasion and deposition on the coral tissue[96,97]. In areas exposed to terrestrial runoff or dredging-related activities, recent evidence suggests that the energetic imbalance produced by the reduction in light availability and symbiotic algae photosynthesis, as well as the process of particle clearance compromises reef-building capacity, coral survivorship and coral reef structure[74,96,98-100]. Moreover, that these responses to water turbidity alone or in combination with other type of stressors may be species-specific and mediated by the duration and intensity of the exposure. Despite the recent advances in knowledge, a holistic approach is still needed to gain a broader understanding of the effects of pollution on the water optical properties, the underwater light climate, and the physiology and ecology of reef corals.

Varadero reef in the southern end of the Caribbean, at the mouth of the Cartagena Bay, Colombia, is exposed to a turbid plume of water originating from a man-made channel[101]. As a result of major rectification works between the 1920's and 1980's[102], the Dique channel delivers large

freshwater discharges (8,833 m^{-3} s^{-1}) with high sediment load (23,906 t d^{-1}) into the Cartagena Bay[103]. The permanence of this reef under suboptimal environmental conditions provides a unique opportunity to explore the physiological and ecological consequences on reef corals produced by the progressive degradation of the water optical properties. Taking a holistic approach, we investigated these effects using as a proxy the coral species *Orbicella faveolata*, an ecologically dominant and major reef-builder in the Caribbean. We hypothesize that the reduction in light penetration as a result of water pollution have important effects on the physiology and energy balance of *O. faveolata* colonies, which in turn affect the vertical distribution and population structure of this and potentially other symbiotic coral species. A better understanding of these effects is essential for predicting future impacts associated with coastal development and terrestrial runoff and for the implementation of more effective management efforts seeking to control local key stressors on coral reef ecosystems.

Material and Methods

Site selection criteria

Two sites within the Cartagena Reef System with contrasting water optical properties but similar total light exposure were considered: a turbid-water reef "Varadero", close to the Dique channel outlet (10° 18' 23.3'' N, 75° 35' 08.0'' W), and a clear-water reef located 21 km southwest of Varadero within the marine protected area Parque Nacional Natural Corales del Rosario y San Bernardo, hereafter referred as "Rosario" (10° 11' 12.1'' N, 75° 44' 43.0'' W) (Figure **2-1**). The Dique is a man-made distributary channel that diverges from the Magdalena River, the largest river system of Colombia and major contributor of continental fluxes into the Caribbean[103]. The shallow portion of Varadero reef is in good condition in terms of coral cover (up to 50-60%)[101], despite its proximity to the Dique outlet.

Preliminary analyses of the vertical diffuse attenuation coefficient for downwelling irradiance (K_d) obtained by measuring light intensities across depths using the cosine-corrected PAR sensor of a Diving PAM (Walz, Germany), indicated that the total light exposure at 3.5 m in Varadero and at 12 m in Rosario was similar. Temperature at these depths was recorded every 30 min between November 2016 and July 2017 with HOBO pendant dataloggers (UA-002-64, Onset Computer Corporation, USA). A small (0.27 ºC) but significant difference in temperature was detected between sites (29.15 ± 1.22 (daily mean ± SD) in Varadero and 28.88 ± 0.89 °C in

Rosario; $H_{(1)} = 5.58$, $p = 0.018$). However, the resulting variation in *O. faveolata* metabolic rates based on the scaling quotient of temperature $(Q_{10})^{21}$ is estimated to be negligible (<4%).

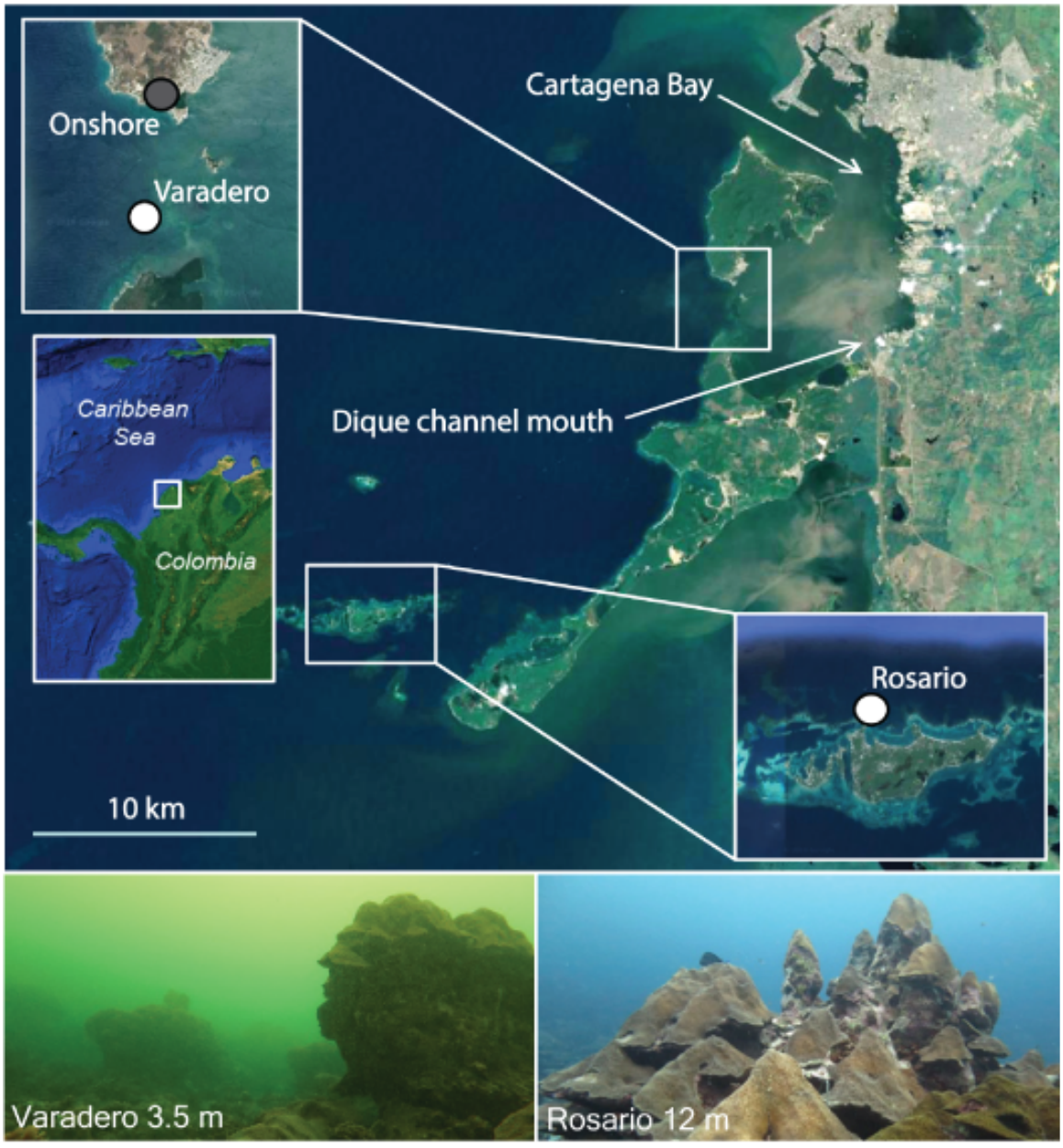

Figure **2-1**: Study sites with contrasting exposure to the Dique plume. Varadero is located ~6 km west of Dique mouth, and Rosario 21 km southwest of Cartagena Bay (white circles). Surface irradiance was measured onshore close to Varadero (grey circle) to estimate K_d variation. Arrows indicate the location of Cartagena Bay and Dique channel mouth. Lower panels illustrate a general view of the study sites. Map data: Google, Maxar Technologies.

Coral Sampling

In October of 2016, small coral fragments (~10 cm^2) were collected from the edge of 15 apparently healthy *Orbicella faveolata* colonies at each site minimizing sampling impacts. Source colonies were chosen randomly at a constant depth of ~3.5 m in Varadero and ~12 m in Rosario, where total light exposure was similar. Coral colonies can produce internal light gradients depending on colony geometry which affect the photoacclimation status[51,71]. In order to eliminate this effect and obtain a constant photoacclimation mediated by depth and downwelling irradiance, coral fragments were fixed in horizontal position to PVC panels with non-toxic epoxy (Z-Spar A-788 epoxy). Corals were allowed to heal and fully recover for seven months at the same depth of collection, after which a subsample from the survivors (12 in Rosario and 15 in Varadero) was used for physiological analysis and genetic identification of algal symbionts.

Irradiance measurements

Irradiance was monitored every ten minutes for one year (November 2016 - November 2017) at each site with cosine-corrected light sensors (Odyssey PAR, Dataflow systems, New Zealand), previously cross-calibrated against a manufacturer-calibrated quantum sensor (LI-1400, LI-COR, USA). The light sensors were cleaned and downloaded periodically (every two months or less). Visual inspections at each visit showed that sediments and biofouling were not covering the sensors, potentially related to the type of sediments of the Dique plume (mainly fine silts and clays) which tend to remain suspended in the water column[104]. Even if the potential interference of sediments in the sensor's signal was low, a linear regression on the data was used for correcting cumulative signal attenuation.

Spatiotemporal variation of water optical properties

To estimate the variation of the water optical properties resulting from the Dique plume dynamics, light data recorded underwater were compared with data simultaneously recorded onshore close to Varadero (Figure **2-1**). With this array, we isolated the variations of irradiance associated with the plume from variations due to cloud coverage. The irradiance synchronously

recorded onshore and underwater was used to estimate instantaneous values of K_d with the equation:

$$K_d = \ln(E_z/E_0) / -z \qquad \text{(Equation 2-1)}$$

where E_z is underwater irradiance, E_0 is onshore irradiance, and z is the depth of the underwater sensor (3.5 m). Only data recorded between 7:00 and 17:00 was used. The analysis was performed over one-hour averages, smoothing out anomalies due to differences in cloud coverage between sites at short time intervals. Occasional failures of either sensor reduced the amount of time intervals that could be used to estimate K_d's, leaving a total of 86 days of usable data.

The vertical spectral diffuse attenuation coefficient for downwelling irradiance ($K_d\,\lambda$) was estimated by modifying the methodology of Maritorena and Guillocheau [12]. A mini-spectrophotometer (Flame T-UV-VIS-ES, Ocean Optics, USA) connected to a cosine-corrected sensor through a 30 m fiber optic cable (Avantes, Apeldoorn, The Netherlands) was used to measure irradiance at ocean surface and at several depths at each site. A bubble level was used to keep the light sensor horizontal, avoiding divers or boat shading. $K_d\,\lambda$ was calculated based on the change of underwater light spectra relative to surface. The spectral sensitivity of the instrument and the attenuation of the fiber optic were accounted for by normalizing the surface spectra against a traceable solar spectra reference[105].

Symbiont identity

Coral samples were stored at -80 °C prior to processing. 50 µl of DNA was extracted from each sample (n = 15 in Varadero; n = 12 in Rosario) using the MoBio Powersoil DNA Isolation Kit (MoBio Laboratories, Carlsbad, California). Two-stage amplicon PCR was performed on the Internal Transcribed Spacer 2 (ITS2) rRNA marker gene. We used modified versions of the itsD and its2rev2[106], including universal primer sequences that are required for Illumina MiSeq amplicon tagging and indexing. The PCR amplification was structured as follows: 2 min of denaturation at 94 °C; 35 cycles of 45 s at 94 °C, 60 s at 55 °C, and 90 s at 68 °C; then finally 7 min at 68 °C. Samples were sequenced using the Illumina MiSeq platform at the DNA Services Facility at the University of Chicago, Illinois. Resulting sequences were submitted to SymPortal for further processing and downstream analyses[107]. Sequences within the Symbiodiniaceae family were identified and separated into genera, formerly "clades"[108], which were further separated into ITS2 type profiles representative of putative Symbiodiniaceae taxa[107]. Sequence variants

occurring in less than 1% of the sample were omitted in order to remove rare intragenomic variants and sequence artifacts generated by MiSeq sequencing.

Photophysiological responses

Chlorophyll *a* (Chl *a*) fluorescence data were collected *in situ* with a submersible pulse amplitude modulated fluorometer (Diving-PAM, Walz, Germany). On cloudless days (n = 3 at each site), we quantified PSII photochemical yields in algal symbionts of 15 colonies randomly distributed near the experimental sites at constant depths (~3.5 m Varadero and ~12 m Rosario). Measurements were taken in the horizontal-uppermost part of colonies to avoid interference of intra-colony light gradients. The effective quantum yield ($\Delta F/F_m'$) of photosystem II (PSII) was recorded at local noon and the maximum quantum yield (F_v/F_m) of PSII at dusk or dawn. The maximum excitation pressure over PSII (Q_m) was calculated following Iglesias-Prieto, et al. [43]:

$$Q_m = 1 - \left[\left(\Delta F/F_m' \text{ at noon}\right) / \left(F_v/F_m \text{ at dusk}\right)\right] \qquad \text{(Equation 2-2)}$$

Chl *a* was extracted from tissue slurries (n = 7 Varadero; n = 8 Rosario) obtained with an air gun connected to a scuba tank and subsequently homogenized with a Tissue-Tearor Homogenizer (BioSpec Inc, USA). Pigment extraction was performed in acetone/dimethyl sulfoxide (95:5 vol/vol). Chl *a* density was estimated spectrophotometrically (n = 3 per sample) with a modular spectrometer (Flame-T-UV-VIS, Ocean Optics Inc., USA) using the equations of Jeffrey and Humphrey [109]. The specific absorption coefficient of Chl *a* ($a^*_{Chl\,a}$) was calculated according to Enríquez, et al. [110]:

$$a^*_{Chl\,a} = (D_{675}/\rho) * \ln(10) \qquad \text{(Equation 2-3)}$$

where D_{675} is the estimated absorbance value of corals at 675 nm, calculated from reflectance (R) measurements as [$D_{675} = \log(1/R_{675})$], and ρ is the pigment content per projected area (mg Chl *a* m^{-2}). Coral reflectance was measured using a similar optical set-up as Vásquez-Elizondo, et al. [111]. Coral surface area for these and other metrics was determined with the aluminum foil technique[112]. Cell counts to estimate algal density and cell pigmentation were not reliable due to improper sample preservation and not included in any analysis.

Photosynthetic parameters were obtained from PE (photosynthesis vs irradiance) curves performed under laboratory conditions in a gradient of artificial light. Incubations (n = 8 in Varadero; n = 6 in Rosario) were performed in a custom-made acrylic chamber with four

hermetic compartments (~650 ml each) filled with filtered seawater (0.45 µm) under constant agitation. Temperature was maintained at 28 °C with an external circulating water bath (Isotemp, Fisher Scientific). Ten levels of irradiance previously measured with a Diving-PAM light sensor were supplied at 10-min intervals with four 16 W LED warm white bulbs (UL PAR38, LED Wholesalers Inc, USA) controlled with a custom-made software in continuous-mode. The range of light intensity covered was 0 to ~1400 µmol quanta m^{-2} s^{-1}. Oxygen concentrations were measured with a 4-channel fiber-optic oxygen meter system (FireSting, Pyroscience). Parameters were calculated following Iglesias-Prieto and Trench [39].

Ecological survey

We performed ecological surveys to estimate the condition of *O. faveolata* populations. Random dives near each site allowed us to define the vertical distribution ranges of the species. Colony abundance and percentage of old mortality were recorded across five sequential 10x1 m belt transects deployed perpendicular to the reef slope at six depths in Varadero (2, 3, 4.5, 6, 7.5 and 9 m) and Rosario (3, 5, 7, 9, 13 and 17 m). The percentage of old mortality was estimated following the AGRAA protocol (*i.e.*, coral skeleton is no longer white and has been lost or covered by epibenthic organisms)[113]. Completely dead colonies were excluded from surveys due to species identification uncertainty.

Autotrophic capacity

Variation of the phototropic contribution of algal symbionts to the energy requirements of *O. faveolata* colonies across depths was estimated using as a proxy the daily integrated photosynthesis to respiration [P:R] ratios. This index of autotrophic capacity was estimated using the PE curve parameters (mean values) and light availability across depths, calculated based on the oscillation of estimated K_d's (derived from equation 1). Daily integrated photosynthesis (P^{g}_{day}) was calculated with a hyperbolic tangent function[54]:

$$P^{g}_{day} = \int_0^{24} \left[P^{g}_{max} \tan h\left(\alpha E_z / P^{g}_{max}\right)\right] dE_z \qquad \text{(Equation 2-4)}$$

where P^{g}_{max} is maximum gross photosynthesis, α is photosynthetic efficiency, and E_z is the estimated irradiance at depth z. The daily integrated respiration (R_{day}) was calculated with an equation modified from Chalker [114]:

$$R_{\mathrm{day}} = \int_0^{24}\left[\left[\Delta R_d \ \tanh\left(E_z/E_{\mathrm{k}}\right)\right] + R_{\mathrm{d-pre}}\right] dE \qquad \text{(Equation 2-5)}$$

where ΔR_{d} represents the difference between the post- and pre-illumination respiration rates, E_k is saturating irradiance, and $R_{\mathrm{d\text{-}pre}}$ is pre-illumination respiration rate. We assumed a light-associated asymptotic increase of the respiratory activity until reaching a maximum determined by E_{k}. This assumption is based on evidence that indicates that respiration rates in corals are light-driven and closely coupled with the internal oxygen concentration[4,115].

Results

Spatiotemporal variation of water optical properties

Analysis of K_{d}'s obtained at the beginning of the study with a Diving-PAM light sensor indicated a strong stratification of the water column in Varadero (Figure **2-2a**). The stratification was characterized by a superficial layer of ~1 m with an extremely high K_{d} (1.93 ± 0.26 m^{-1}, mean ± SD), and a clear subsurface layer with significantly lower K_{d} (0.31 ± 0.11 m^{-1}) ($t_{(7)} = 15.31$, $p < 0.01$). No noticeable stratification was detected in Rosario, which revealed a monotonic K_{d} (0.16 ± 0.01 m^{-2}) (Figure **2-2a**). The estimated K_{d}'s based on the synchronous oscillation of onshore and underwater irradiance were 0.92 ± 0.26 m^{-1} and ranged between 0.38 and 1.95 m^{-1} (Figure **2-2b**).

Analyses of $K_{\mathrm{d}}\,\lambda$ indicated distinctive light scattering and absorbing characteristics of dissolved and particulate matter in the water at each site (Figure **2-2c**). Varadero's high variability of $K_{\mathrm{d}}\,\lambda$ (*i.e.*, wide confidence intervals) (Figure **2-2c**) was consistent with the strong stratification (Figure **2-1a**) and the temporal variation of K_{d} (Figure **2-2b**). $K_{\mathrm{d}}\,\lambda$ evidenced two spectral regions with contrasting characteristics. One below ~600 nm with increasing attenuation toward shorter wavelengths in Varadero and low attenuation in Rosario, attributed to light absorption of dissolved organic material of continental origin[12]. And a spectral region above 600 nm with nearly constant properties despite differences in attenuation magnitude among sites, attributed to light attenuation due to scattering by particulate matter with small effect on spectral quality (Figure **2-2c**). The estimated attenuation due to absorptance of dissolved organic matter obtained from a differential normalized spectrum (Figure **2-2d**), demonstrated the high concentration of dissolved organic matter in Varadero associated with the Dique plume and its critical role in modifying the underwater light quality.

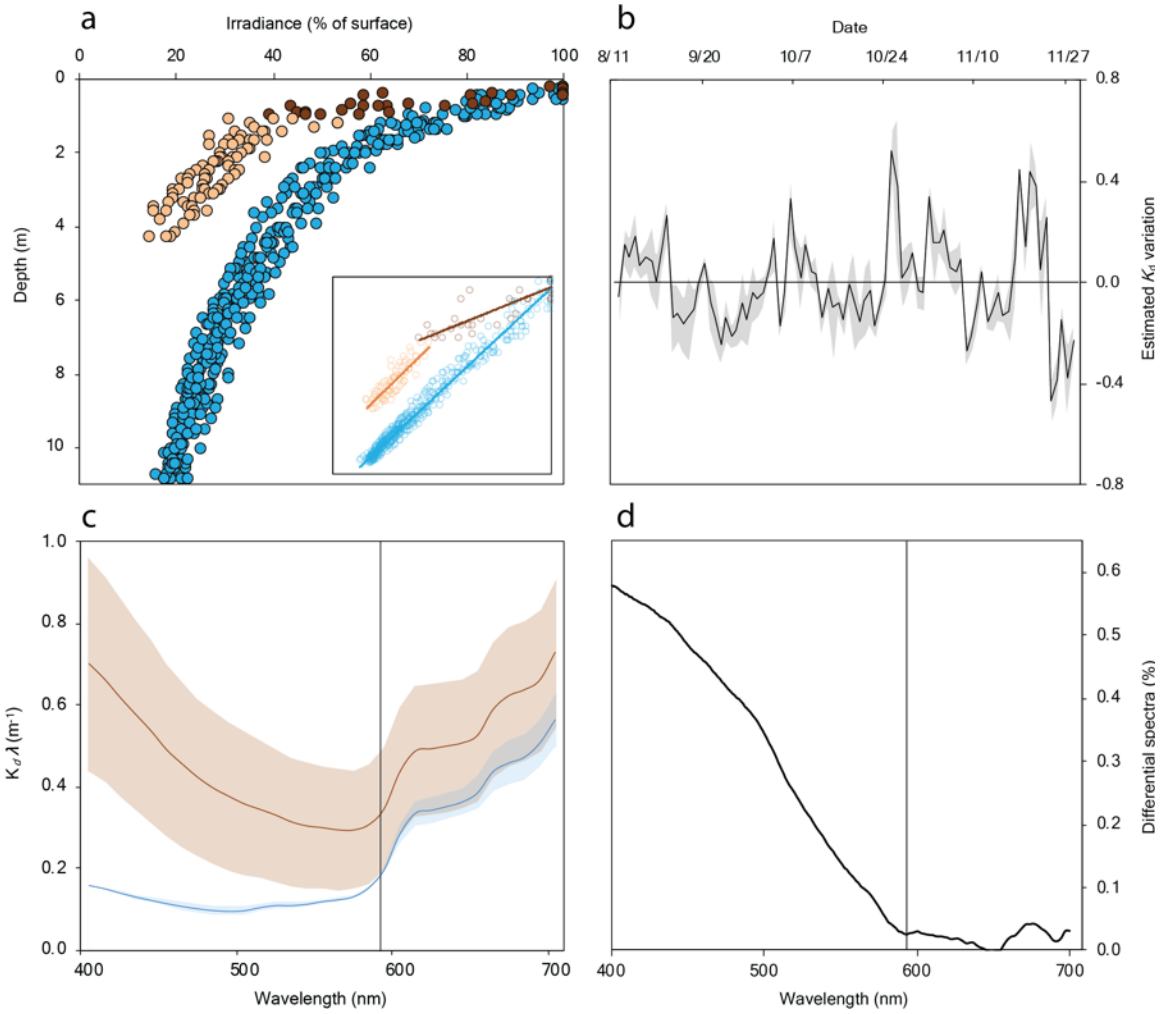

Figure **2-2**: Variation of underwater light climate and water optical properties. **a** Strong stratification of the water column in Varadero characterized by a superficial layer with high K_d (1.93 ± 0.26 m^{-1}, dark-brown) and a clearer subsurface layer with low K_d (0.31 ± 0.11 m^{-1}, light-brown), compared with Rosario monotonic K_d (0.16 ± 0.01 m^{-1}, blue). The insert shows light data distribution with depth in log-scale. **b** Temporal variation of mean daily K_d in Varadero estimated from onshore and underwater irradiance (shaded area represents SD). **c** $K_d\,\lambda$ in Varadero (brown) and Rosario (blue) (shaded areas represent 95% confidence intervals). **d** Estimated light attenuation due to absorptance of dissolved organic matter associated to Dique discharges based on a differential normalized spectrum in Varadero. Vertical line in **c** and **d** separate the two contrasting spectral regions.

Dramatic changes of K_d were detected within and between days (Figure **2-3**), highlighting the variable nature of the water optical properties and underwater light climate associated with the Dique plume dynamics in Varadero. On average, the daily integrated irradiance was 7% lower in Varadero than in Rosario (2.03 ± 1.32 and 2.17 ± 0.91 mol quanta m^{-2} d^{-1}, respectively) ($H_{(1)}$ =

7.92, $p < 0.05$). Prevalent irradiance at both sites was consistent with low-light reef environments[66,116].

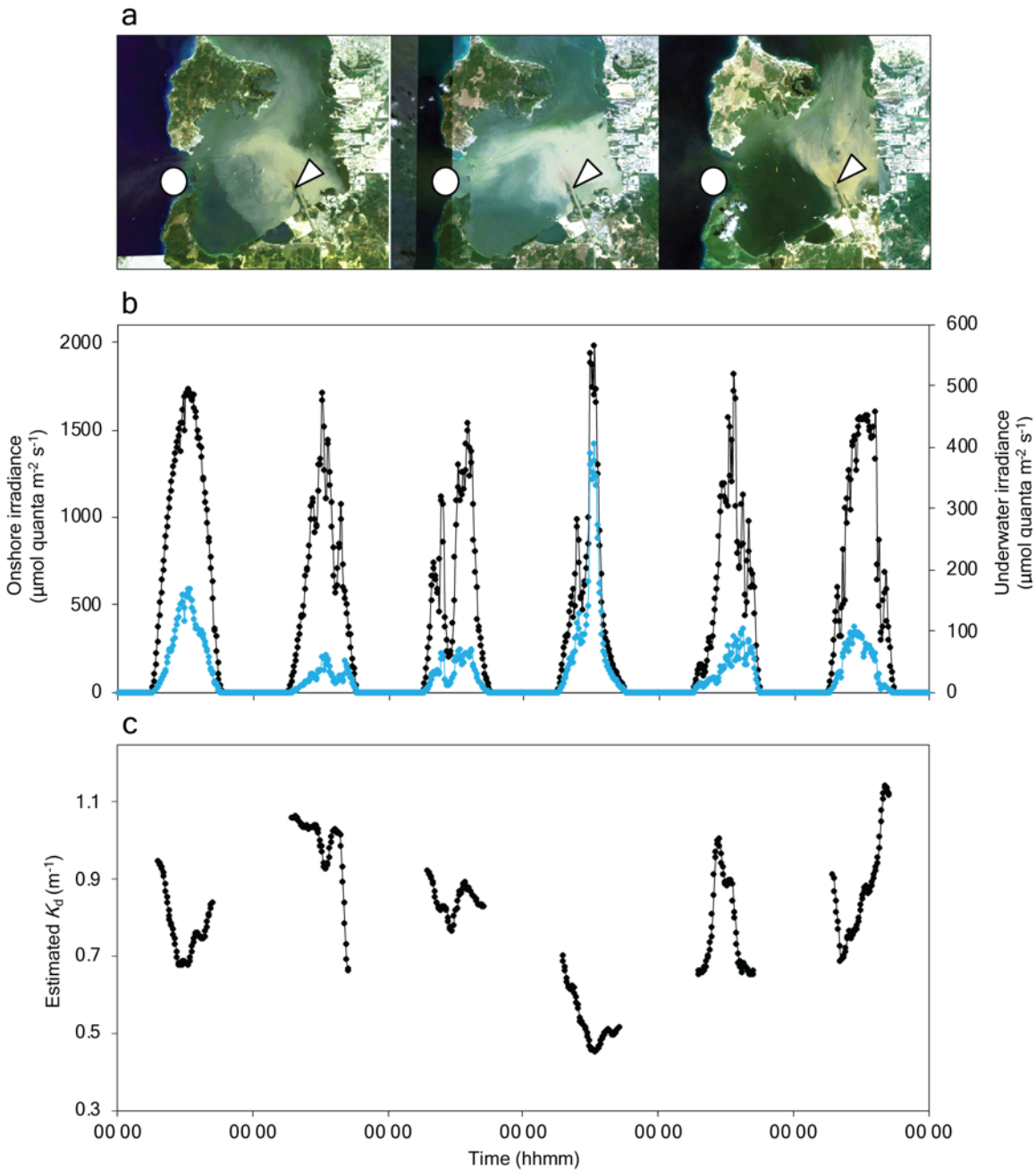

Figure **2-3**: Effect of Dique plume dynamics on K_d. **a** Satellite images illustrating contrasting spatial patterns of the plume, signaling the location of Varadero (circle) and the Dique mouth (arrow). **b** Oscillation patterns of onshore (black line) and underwater (blue line) irradiance on six random days. **c** K_d variation estimated from onshore and underwater irradiance.

Symbiont identity

Analyses of Internal Transcribed Spacer 2 (ITS2) rRNA sequences identified distinctive ITS2 profile combinations diagnostic of five separate Symbiodiniaceae genotypes. One belonged to the genus *Symbiodinium* (ITS2 type A3), one to *Breviolum* (ITS2 type B1) and three to *Cladocopium* (ITS2 types C7, C7/C12c, C3ee/C21/C3an) (Figure **2-4**). The community structure of algal symbionts in terms of ITS2 profiles composition was different between sites ($p = 0.001$, PERMANOVA on Bray-Curtis matrix). In Varadero, a single *Cladocopium* genotype (ITS2 type C3ee/C21/C3an) was present in all colonies sampled and in nearly half of them it was the only dominant symbiont (abundance of >80%). A *Symbiodinium* genotype (ITS2 type A3) was also present in 67% of colonies. The symbiont diversity in coral samples from Rosario was more diverse and included representatives of the five different genotypes. *Cladocopium* ITS2 type C7/C12c and *Symbiodinium* ITS2 type A3 were the most abundant symbionts in corals from Rosario, detected respectively in 50% and 42% of the colonies. A *Breviolum* genotype (ITS2 type B1) was detected in half of the samples but in low background levels (abundance of <13%). *Cladocopium* ITS2 type C3ee/C21/C3an, also detected in Varadero, and *Cladocopium* ITS2 type C7 were present in a few corals from Rosario (17% and 25%, respectively) being the only dominant symbiont. Interestingly, the three *Cladocopium* genotypes detected in Rosario never occurred together on the same colony.

Photophysiological responses

Photosynthetic parameters derived from the PSII photochemical yield of symbionts (F_v/F_m, $\Delta F/F_m'$ and Q_m) and host pigmentation (Chl *a* content and $a^*_{Chl\ a}$) were significantly different between sites. Parameters derived from the photosynthetic potential (α, E_c, E_k, R_d, P_{max} and $1/\Phi_{max}$) and corals capacity to absorb light (A_{PAR}) were non-significantly different (Table **2-1**). F_v/F_m values (0.669 ± 0.019 and 0.676 ± 0.012 in Varadero and Rosario, respectively) differed by 1% ($t_{(74)} = 2.26$, $p = 0.027$). Values of $\Delta F/F_m$' and Q_m (0.579 ± 0.052 and 0.610 ± 0.033, and 0.135 ± 0.062 and 0.097 ± 0.051 in Varadero and Rosario, respectively), varied by 5% ($t_{(75)} = 3.38$, $p = 0.001$) and 28% ($t_{(84)} = -3.09$, $p = 0.003$), respectively. Estimated values of $1/\Phi_{max}$ (11.24 ± 1.87 and 11.62 ± 3.16 quanta O_2^{-1} in Varadero and Rosario, respectively) were lower than previous reports [117,118] and close to minimum practical limits of ~10-12 quanta O_2^{-1} [119].

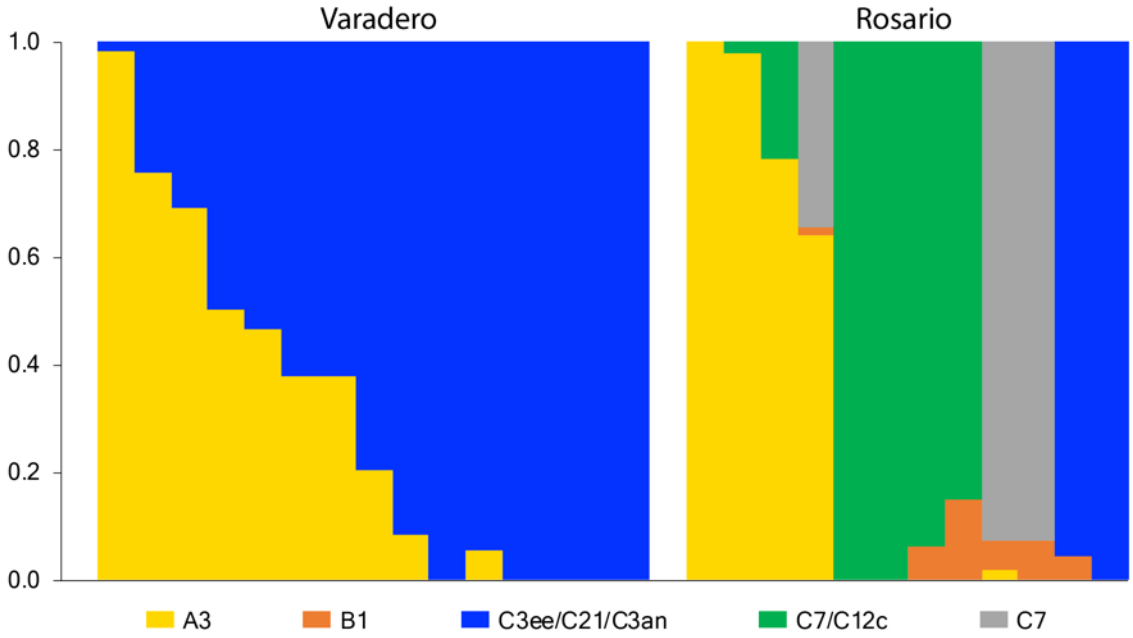

Figure **2-4**: Predominant Symbiodiniaceae ITS2 profiles associated to corals from Varadero and Rosario. Each column of stacked bars represents one sample, with bar heights within each column representing the relative abundance of sequences.

Chl *a* density was significantly higher ($t_{(10)} = -5.95$, $p < 0.001$) in corals from Varadero compared to Rosario (195.27 ± 37.61 and 95.07 ± 25.54 mg Chl *a* m^{-2}, respectively). Changes in Chl *a* density resulted in significant variations of $a^*_{Chl\ a}$ (0.013 ± 0.002 and 0.031 ± 0.012 m^2 mg Chl a^{-1} in Varadero and Rosario respectively, $H_{(1)} = 10.5$, $p = 0.001$). Comparative analyses of changes in $a^*_{Chl\ a}$ as a function of Chl *a* content indicate a relatively steady light harvesting efficiency despite larger differences in pigment content in corals from Varadero. In contrast, reduced Chl *a* content variation in Rosario resulted in more dramatic changes of the effective absorption cross section of algal pigments. Our data provide no clear evidence that these differences were associated with distinctive Symbiodiniaceae composition. No significant differences were found in light absorption capacity (A_{PAR}) and photosynthetic descriptors normalized per unit area (α, E_c, E_k, R_d and P_{max}) between sites (Table **2-1**).

Table **2-1**: Photoacclimation parameters of *O. faveolata* in Varadero at 3.5 m and Rosario at 12 m

Parameter [units]	Definition	Varadero	Rosario	Statistic
F_v/F_m [Dimensionless]	Maximum quantum yield of PSII at dusk	0.669 ± 0.019 (45)	0.676 ± 0.012 (44)	$t_{(74)} = 2.26$, $p = 0.027$
$\Delta F/F_m'$ [Dimensionless]	Effective quantum yield of PSII at noon	0.579 ± 0.052 (45)	0.610 ± 0.033 (44)	$t_{(75)} = 3.38$, $p < 0.001$
Q_m [Dimensionless]	Maximum excitation pressure over PSII	0.135 ± 0.062 (45)	0.097 ± 0.051 (44)	$t_{(84)} = -3.09$, $p < 0.001$
A_{PAR} [Dimensionless]	Light absorptance	0.87 ± 0.02 (8)	0.88 ± 0.04 (8)	$t_{(11)} = 0.49$, $p = 0.632$
Chl *a* [mg Chl *a* m^{-2}]	Chlorophyll *a* content per area	195.27 ± 37.61 (7)	95.07 ± 25.54 (8)	$t_{(10)} = -5.95$, $p < 0.001$
$a^*_{Chl\ a}$ [m^2 mg Chl a^{-1}]	Chlorophyll *a* specific absorption coefficient	0.013 ± 0.002 (7)	0.031 ± 0.012 (8)	$t_{(7)} = 4.35$, $p = 0.003$
E_c [µmol quanta m^{-2} s^{-1}]	Compensating irradiance	88.84 ± 17.60 (8)	88.11 ± 15.20 (6)	$t_{(11)} = -0.08$, $p = 0.935$
E_k [µmol quanta m^{-2} s^{-1}]	Saturating irradiance	**217.88 ± 26.60 (8)**	210.18 ± 41.28 (6)	$t_{(8)} = -0.4$, $p = 0.7$
R_d [µmol O_2 m^{-2} s^{-1}]	Dark respiration rate	**3.40 ± 0.30 (8)**	3.43 ± 0.62 (6)	$t_{(6)} = -0.1$, $p = 0.92$
P_{max} [µmol O_2 m^{-2} s^{-1}]	Maximum gross photosynthetic rate	**5.04 ± 1.16 (8)**	4.76 ± 1.31 (6)	$H_{(1)} = 0.27$, $p = 0.606$
α [quanta O_2^{-1}]	Photosynthetic efficiency	**0.039 ± 0.006 (8)**	0.041 ± 0.014 (6)	$t_{(6)} = 0.22$, $p = 0.834$
$1/\phi_{max}$ [quanta O_2^{-1}]	Minimum quantum requirement	11.24 ± 1.87 (8)	11.62 ± 3.16 (6)	$t_{(7)} = 0.27$, $p = 0.798$

Ecological survey

O. faveolata vertical distribution ranged between 2 and 9 m in Varadero, and 3 and 17 m in Rosario. Varadero had both higher colony density (3.20 ± 2.85 colonies $transect^{-1}$) and coral cover (4.46 ± 4.57 m^2 $transect^{-1}$) than Rosario (1.70 ± 1.18 colonies $transect^{-1}$ and 4.20 ± 5.48 m^2 $transect^{-1}$, respectively). The highest abundance (38% of total colonies) occurred at 4.5 m in Varadero and at 9 m (33%) in Rosario. In Varadero, the lowest partial colony mortality occurred at 2 m (7.5 ± 3.5%) and the highest at 9 m (73.3 ± 26.4%). In Rosario, the lowest mortality occurred at the maximum depth (5.0 ± 12.2% at 17 m) and the highest at an intermediate depth (73.3 ± 20.8% at 5 m) (Figure **2-5**). Depth and mortality had a strong exponential relationship in Varadero ($R^2 = 0.77$, $p<0.01$) and a non-significant linear ($R^2 = 0.43$, $p = 0.16$) or exponential ($R^2 = 0.33$, $p = 0.23$) relationship in Rosario.

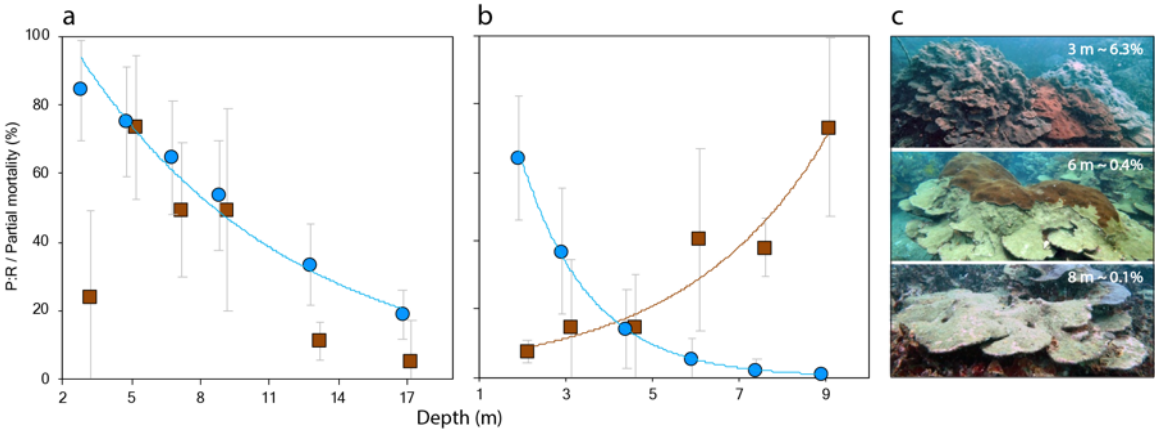

Figure **2-5**: Productivity and mortality of *O. faveolata* across depths. Partial mortality (brown squares) and daily integrated P:R ratios (%, blue circles) in Rosario (**a**) and Varadero (**b**). Values correspond to mean ± SD. Exponential regressions were used to fit the data (only significant relationships are depicted). **c** Mortality patterns across depths in Varadero, indicating the % surface light at each depth based on the mean estimated K_d.

Autotrophic capacity

The index of autotrophic capacity of *O. faveolata* colonies from Varadero suggested a variable phototrophic contribution of algal symbionts to the metabolic demand of coral holobionts, both spatially (across depths) and temporally, as a consequence of changes in light availability. At 2 m depth, the index had a mean of 0.64 ± 0.18 (SD). On days with increased light penetration in the water column (*i.e.*, low K_d) the index increased up to 0.99 while on days with reduced light penetration it dropped to 0.20. At 9 m, the maximum depth where living *O. faveolata* colonies were found in Varadero, the index had a mean of 0.01 ± 0.01 and oscillated between 4.49 x 10^{-6} and 0.07 (Figure **2-5**). A strong, negative correlation was found between colonies partial mortality and the index of autotrophic capacity (Spearman r_s = -0.94, p = 0.005). The coefficient of determination of an exponential regression indicated that the autotrophic capacity explains 78% of the mortality variation across depths in *O. faveolata*.

In Rosario at 3 m and 17 m, the local vertical limits of *O. faveolata*, the index of autotrophic capacity had a mean of 0.84 ± 0.14 and 0.19 ± 0.07, respectively. The index' range of variation was 0.20-0.98 and 0.02-0.27 in the upper and lower depth limits, respectively, depending on changes in light availability (Figure **2-5**). Corals from Rosario had significantly higher autotrophic capacity than corals from Varadero both at the upper ($H_{(1)}$ = 73.29, p < 0.001) and

lower ($H_{(1)} = 189.25$, $p < 0.001$) local depth limits. There was no significant correlation between colony partial mortality and the autotrophic capacity of corals from Rosario (Spearman $r_s = 0.60$, $p = 0.208$).

Discussion

We identified three main features of the underwater light climate in the turbid-water Varadero reef: 1) light-limiting conditions due to the strong attenuation generated by particulate matter and dissolved substances concentrated in a superficial layer of water, 2) substantial variation of the underwater light climate in response to fluctuations of water optical properties, and 3) altered spectral composition of light due to the wavelength-selective absorption by organic matter of continental origin[12,52]. These patterns are produced by the freshwater discharges with high sediment load from the Dique channel in the vicinity of the reef. The strong stratification, also reported in previous studies[101,120], results from the different properties of a superficial layer directly affected by the Dique channel discharges and a subsurface clear layer of oceanic waters [104]. This stratification seems to isolate Varadero from the direct influence of the Dique freshwater discharges, but have a critical impact on the underwater light availability.

The variation of the water optical properties in Varadero inferred from the synchronous oscillation of onshore and underwater irradiance explains 81% of the overall temporal variation of underwater light availability. This estimation is in close proximity to irradiance variation in other turbid-water reefs due to suspended solids[50]. Maximum K_d's were higher compared to previous reports at this site[101,121] and other turbid-water reefs[52,99]. The extremes within the K_d range of variation indicate that irradiance can vary by up to two orders of magnitude only due to changes in water optical properties attributed to meteorological conditions affecting the Dique plume dynamics[104,120]. At Rosario, the clear-water site, although the water column was significantly clearer than Varadero, the K_d's for the whole PAR range (0.158 m^{-1}) and towards the blue part of the spectrum (0.160 m^{-1} at 400 nm) were still notably higher compared to other reports in clear waters[12]. This suggests an increased attenuation likely associated with the Dique discharges, highlighting that their influence extend far beyond the channel mouth to this natural protected area.

Our results suggest that *O. faveolata* colonies host distinctive Symbiodiniaceae communities in Varadero and Rosario. Symbiodiniaceae communities were more diverse in corals from Rosario

than in Varadero mainly due to an increased richness of *Cladocopium* genotypes. It is known that *O. faveolata* associates with genetically distinct symbionts from four genera following gradients of irradiance, with combinations of *Symbiodinium, Breviolum* and *Durusdinium* genotypes typically found in high-light environments and *Cladocopium* genotypes in low-light environments[17,19,122]. The greater diversity and abundance of *Cladocopium*, a highly diverse taxa throughout the Caribbean[123], as well as the absence of *Symbiodinium* genotypes in Rosario may indicate the occurrence of coral-algae associations favored by a more predictable low-light environment. While in Varadero, the presence of *Symbiodinium* genotypes in some samples and the reduced diversity of Symbiodiniaceae may be indicators of the strong selective pressure exerted by the turbid plume dynamics on the symbiont communities, similar to previous reports in other turbid marginal reef environments[124].

Low-light phenotypes of *O. faveolata* were found both in Varadero at 3.5m and in Rosario at 12m, which highlights the essential role of the water optical properties on the photoacclimation status and illustrates the constraint of using depth as main proxy. Estimated minimum quantum requirements ($1/\Phi_{max}$) of corals growing at both sites indicate similar light utilization efficiency close to theoretical operational limits of ~10-12 quanta O_2^{-1} [119]. Q_m values close to 0 indicate that even at noon when corals are exposed to maximal irradiance, most PSII reaction centers of symbiotic algae remained open suggesting light-limited photosynthetic rates [43]. Both Q_m and $1/\Phi_{max}$ normally decrease with increasing depth until reaching the minimal practical values, which corresponds to the limits of potential photoacclimation capacity and tolerance range for the symbiosis[43,117]. The values of Q_m and $1/\Phi_{max}$ close to theoretical minimums suggest that the photoacclimation of *O. faveolata* symbionts is close to the limit for maximum efficiency of solar energy utilization and, therefore, the lower vertical distribution limit of the species at each site despite the differences in depth.

Comparative analyses of the parameters derived from the P-E curves indicate that corals at both locations have very similar photosynthetic potential, even when corals from Varadero are occasionally exposed (~10% of days) to supersaturating irradiance. During these periods, irradiance can be almost twice the light saturation point (E_k), representing a potential source of over-excitation of the photosynthetic apparatus that must be dissipated by photoprotective mechanisms. A greater reduction of the quantum yield of photosystem II (PSII) measured at noon ($\Delta F/F_m'$) relative to its maximum value at dusk (F_v/F_m), indicate that corals from Varadero were indeed exposed to a higher irradiance during measurements, compared to Rosario. It must be

stressed, however, that the almost identical values of F_v/F_m between sites indicate similar photochemical energy conversion efficiency of coral symbionts. This suggests that the occasional exposure to higher irradiance in Varadero are not intense enough as to induce a chronic photoinactivation of a population of PSII reaction centers in order to increase the capacity to dissipate excess excitation via non-photochemical quenching[45].

Corals in Varadero had greater Chl *a* content and lower light absorption efficiency of algal pigments than corals from Rosario, potentially associated with other runoff impacts in the water column besides a reduction in light penetration. It is known that the presence of particulate matter and dissolved compounds in the water column can interfere in the coral holobiont metabolism[79,82,95], which may be reflected in the pigment content and/or algal cell density. The potential metabolic interference of nutrient enrichment results in a reduction of $a^*_{Chl\ a}$, indicating that the highly pigmented corals from Varadero are less efficient at collecting light per unit of pigment than corals from Rosario as a result of the "pigment packaging" effect[53]. The nearly constant capacity of corals to absorb ~90% of incident light at both sites indicates that the increased pigmentation in corals from Varadero does not confer them with any additional advantage in terms of light harvesting. Furthermore, the lack of differences among photosynthetic parameters indicates that the light absorbed is also utilized with similar efficiency (per unit area) by corals at both sites. These results suggest that a potential nutrient enrichment linked to Dique discharges does not significantly affect the photosynthetic potential of *O. faveolata*.

The estimated index of photosynthetic potential revealed that the daily phototrophic contribution of algal symbionts to the coral host metabolism is low and highly variable due to the temporal dynamics of water turbidity. The reduction of carbon acquisition through photosynthesis with increasing depth and during exposure to elevated turbidity could potentially be counterbalanced by increasing the heterotrophic energy acquisition, as has been observed in some coral species[79,80]. It should be noted, however, that the Dique plume particles can also represent a stress factor for coral colonies even with lethal effects, particularly if the sediments infer low nutritional value and there is low light availability[74,96,98]. The minimum irradiance at which photosynthesis outweighs respiration (E_c) is estimated to be exceeded only above 6 m, at least for short periods of time. The energetically costly process of coral clearance is expected to be strongly limited below this depth due to the negligible phototrophic contribution of algal symbionts and the metabolic depression of the holobiont. Thus, a potential nutritional benefit obtained by particle

feeding may be insufficient to maintain a positive energy balance due to the costs of particle clearance and acute light energy limitation, mostly below certain depths.

The size of *O. faveolata* colonies in Varadero with diameters exceeding 5 m[101] indicate that these colonies are probably hundreds of years old and that the population was established in Varadero long before the Dique major rectification works between the 1920's and 1980's[102]. The current vertical distribution of this species is restricted to shallower depths (2-9 m) compared not only with Rosario (3-17 m) but also with other clear-water sites in the Caribbean (*e.g.*, 2-20 m in Belize[14] and 3-25 m in Curacao[125]). The compressed vertical distribution, together with the strong correlation between partial colony mortality and the autotrophic capacity of corals from Varadero, suggest the occurrence of a progressive decline of *O. faveolata* population from the bottom to the top of the reef (Figure **2-6**). This vertical "compression" effect has also been reported for the whole coral community in other turbid reefs[100]. The gradual but sustained degradation of the water optical properties in Varadero, firstly due to the Dique channeling works and secondly due to the sustained acceleration of soil erosion along the Magdalena River basin[103], seem to be key factors in the population decline and vertical range contraction of *O. faveolata*.

Most coral reefs will be lost in a few decades unless there is a major scaling-up of management efforts and commitment based on an improved understanding of current ecological processes[126]. Despite the significant steps taken to conserve coral reefs and their ecosystem services, the success of management efforts at large scales is low. In addition, major threats such as global warming keep rising and driving reefs toward the breaking point of collapse[93]. Our findings demonstrate the substantial implications that the progressive degradation of the optical properties of coastal waters globally can have on the physiology and vertical distribution of reef-building corals, which in turn inevitable affect the structure of reef coral communities. Future studies should explore with a holistic approach the gradual changes, both at temporal and spatial scales, in photoacclimation and metabolic responses linked to the disruption of corals energy balance in the increasingly abundant marginal environments. Effective policies seeking to improve water optical properties at local and regional scales should be considered a priority goal for coral reef conservation, a challenge that extends far beyond the limits of the coastal zone environment.

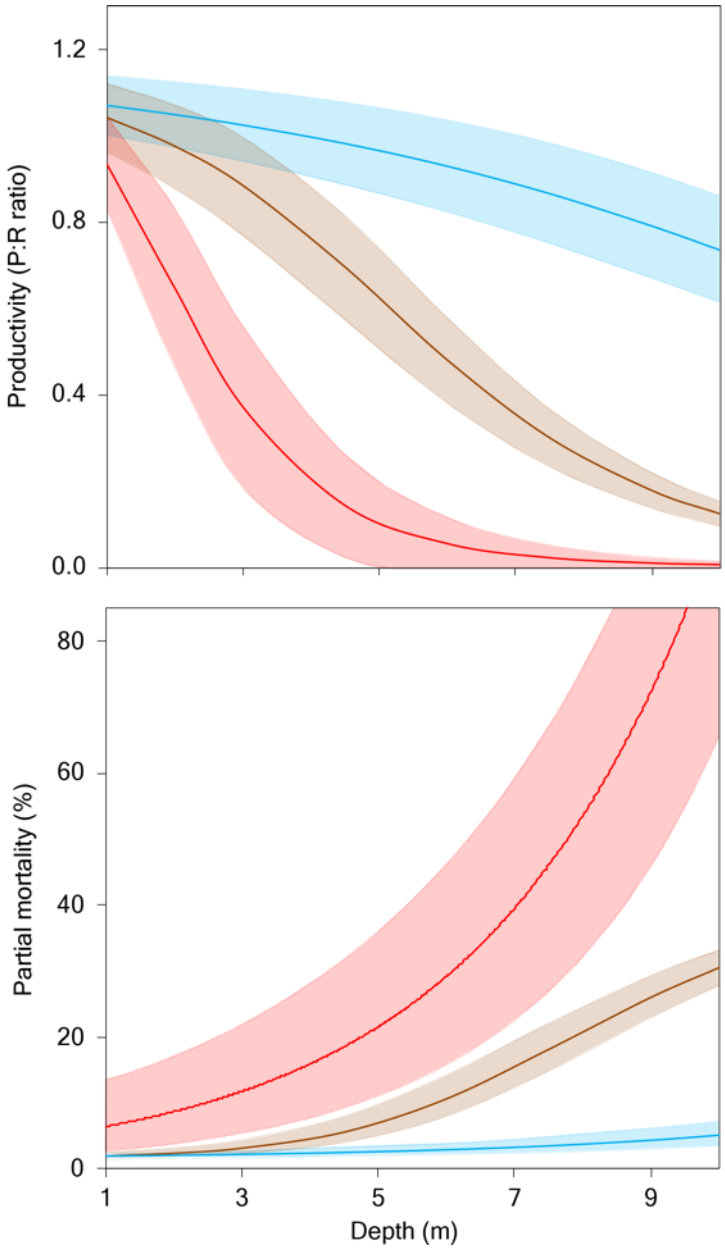

Figure **2-6**: Predicted effect of the progressive degradation of water optical properties on colonies productivity and partial mortality across depths. Top panel: Estimated productivity (daily P:R ratios) with water of different K_d's. Lower panel: Predicted partial colony mortality based on the exponential regression describing the relation between P:R ratios and mortality. Responses were modelled under current K_d variation (red); under persistent low-intensity effect of the Dique plume (lowest estimated K_d, 0.34 m^{-1}) (brown), and under minimal influence of the plume (K_d of Rosario, 0.16 m^{-1}) (blue).

Chapter 3

Linking photoacclimation responses and microbiome shifts between depth-segregated sibling species of reef corals

Manuscript published in: *R. Soc. Open Sci. 9: 211591.*

https://doi.org/10.1098/rsos.211591

Authors

Carlos Prada[1]*[+], Tomás López-Londoño[2]*[+], F. Joseph Pollock[2,3], Sofia Roitman[2], Kim B. Ritchie[4], Don R. Levitan[5], Nancy Knowlton[6], Cheryl Woodley[7], Roberto Iglesias-Prieto[1], Mónica Medina[1]

Affiliations

[1]*University of Rhode Island, Department of Biological Sciences, Kingston, RI 02881, USA*

[2]*Pennsylvania State University, Department of Biology, University Park, PA 16802, USA*

[3]*The Nature Conservancy, Hawai'i and Palmyra Programs, Honolulu, HI 96817, USA*

[4]*University of South Carolina Beaufort, Department of Natural Sciences, Beaufort, SC 29906, USA*

[5]*Florida State University, Department of Biological Science, Tallahassee, FL 32306, USA*

[6]*National Museum of Natural History, Smithsonian Institution, Washington, DC 20560, USA*

[7]*National Oceanic and Atmospheric Administration, National Ocean Service, National Centers for Coastal Ocean Sciences, Hollings Marine Laboratory, Charleston, SC 29412, USA.*

**Corresponding authors*

[+]*Equal contribution.*

Abstract

Metazoans host complex communities of microorganisms that include dinoflagellates, fungi, bacteria, archaea, and viruses. Interactions among members of these complex assemblages allow hosts to adjust their physiology and metabolism to cope with environmental variation and occupy different habitats. Here, using reciprocal transplantation across depths, we studied adaptive

divergence in the corals *Orbicella annularis* and *O. franksi*, two young species with contrasting vertical distribution in the Caribbean. When transplanted from deep to shallow, *O. franksi* experienced fast photoacclimation and low mortality, and maintained a consistent bacterial community. In contrast, *O. annularis* experienced high mortality and limited photoacclimation when transplanted from shallow to deep. The photophysiological collapse of *O. annularis* in the deep environment was associated with an increased microbiome variability and reduction of some bacterial taxa. Differences in the symbiotic algal community were more pronounced between coral species than between depths. Our study suggests that these sibling species are adapted to distinctive light environments partially driven by the algae photoacclimation capacity and the microbiome robustness, highlighting the importance of niche specialization in symbiotic corals for the maintenance of species diversity. Our findings have implications for the management of these threatened Caribbean corals and the effectiveness of coral reef restoration efforts.

Introduction

Understanding how microbial biodiversity interacts with their hosts' physiology is essential for understanding animal ecology and evolution[127]. Microbial communities often influence their host's physiology to cope with environmental variation across habitats[128]. Reef-building corals (Cnidaria: Scleractinia) form a symbiotic association with dinoflagellates, which allow corals to thrive on the ocean's euphotic zone along a strong depth-mediated light gradient[7]. Corals living at different depths possess distinctive physiological and morphological traits to optimize energy acquisition which results from genotypic and phenotypic variation within and between coral species[51,129]. Coral colonies at different depths may host distinctive symbiotic algae with contrasting photoacclimation capabilities that grant their hosts the ability to thrive in certain light environments[17,20]. Because of these differences in photoacclimation and the prevalence of specific associations with coral hosts, zonation by light has been regarded as a primary form of niche partitioning in symbiotic corals[43].

While the influence of different species of symbiotic algae on the ecophysiology of reef-building corals has been studied, the effect of other coral-associated microorganisms is less well known, especially across depth-segregated species[130,131]. However, the interest in coral-associated microbes and their roles in maintaining health and preventing diseases has increased substantially[132,133]. From an eco-evolutionary perspective, the evidence suggests that coral-associated bacterial assemblages can be highly variable, although "footprints" of unique

microbial assemblages appear to be mediated by a combination of host species and local environmental conditions[130,134]. These patterns indicate that bacterial communities, like photosynthetic dinoflagellates, could also be spatially structured and segregated along environmental gradients.

Recently diverged coral species that differ in their vertical distribution are ideal systems to study the microbiota-animal relationship as a potential basis for habitat specialization. The *Orbicella* species complex, dominant in Caribbean reefs, was regarded as one species with ecotypic variation, but recent research revealed three species partially segregated by depth[13,15,16]. *O. annularis* (Ellis and Solander, 1786) forms disjunct columns with senescent edges, being consistently found in shallow-waters between 1 m and ~20 m. *O. franksi* (Gregory, 1895) forms irregular mounds and plates and is typically found deeper than its two sibling species (up to depths of 60 m). *O. faveolata* (Ellis and Solander, 1786) forms massive mounds and can partially overlap with both *O. annularis* and *O. franksi* habitats[13,135]. The three *Orbicella* species are closely related with incomplete lineage sorting across nuclear and mitochondrial markers[15]. The symbiotic dinoflagellate communities[17,19] as well as the photobiology of this species complex have been extensively studied[20,21], enabling the identification of important differences mediated by environmental gradients. The *Orbicella*-associated bacterial communities have also been examined[121,132]. Therefore, this coral species complex offers an ideal system for the study of how species specialize to live in different habitats through adaptive divergence.

Using a reciprocal transplant experiment between shallow and deep environments in Bocas del Toro (Caribbean Panama), we studied adaptive divergence between the two youngest sister species with the most contrasting vertical distribution within the *Orbicella* species complex, *O. annularis* and *O. franksi*. We surveyed colonies for survivorship and characterized the algal symbiont and microbial communities across habitats. We also evaluated if these recently diverged species have also diverged physiologically along depth-mediated light gradients. Our findings suggest that despite being so young (< 500K)[136], these two sister species have diverged in photoacclimation capabilities and microbial symbionts to maximize efficiency in their own light environments.

Materials and Methods

Reciprocal transplantation

To study the effects of depth and light in *O. annularis* and *O. franksi,* 74 unique genotypes (44 of *O. franksi* and 30 of *O. annularis*) were reciprocally transplanted between shallow and deep environments at Bocas del Toro, Panama (latitude: 9.327222, longitude: -82.203889). The study site is located on the slope of a relative narrow reef protected on all sides by islands and has been monitored for coral spawning for two decades[16]. This location is ideal to study adaptation across depths because the vertical distribution of these species is compressed toward shallow depths compared to other sites in the Caribbean[14,125], although maintaining the typical vertical zonation pattern (*O. annularis* in shallow-water between 2.5 and 6 m with greatest abundance at 3 m, and *O. franksi* in deeper-water between 3 and 8 m with greatest abundance at 6 m[16]).

In September 2014, fully pigmented coral clonemate fragments (~5 cm in diameter) were collected from the edges of *O. franksi* colonies (n = 44 donor colonies) and vertically oriented colonies of *O. annularis* (n = 30 donor colonies), each donor colony being a different genotype (74 unique genotypes in total). Coral fragments were collected from two depths in which each species was abundant: shallow for *O. annularis* (3–4 m) and deep for *O. franksi* (7–8 m). Species identification was performed based on morphological features[13], and represented different genotypes following the multilocus genotyping work conducted by Levitan et al.[16]. Genotypic identity was indicated with unique ID tags attached to each colony. Coral fragments from each species were initially transplanted to polyvinyl chloride (PVC) panels placed near the original depth of collection (3.5 m and 9.5 m) where they were left to heal and acclimate for one week. Subsequently, *O. annularis* colonies were transplanted from shallow to shallow (S-S) (n = 27) and shallow to deep (S-D) (n = 30). Similarly, *O. franksi* colonies were transplanted from deep to shallow (D-S) (n = 44) and deep to deep (D-D) (n = 28). The number of fragments transplanted to native environments was lower compared to the ones transplanted to opposite depths because we expected lower mortality in the native environments. We, however, reciprocally transplanted only unique genotypes.

To test for differential mortality across depths, we visually inspected colonies six months after transplantation in March 2015. One detached individual from *O. annularis* transplanted deep was discarded from all subsequent analysis. A one-tailed Fisher exact test was used to assess differences in survivorship among sites. To standardize the fitness (*i.e.,* survival) advantage on

the original depth over the opposite depth for each species, differences in fitness were divided over the average fitness on each particular habitat[137].

Samples were collected in accordance with local regulations under CITES permits PWS2014-AU-002155 and 12US784243/9 and Panama permit number SE/A-94-13.

Environmental parameters

To characterize the effect of the water optical properties on light availability across depths, we measured the diffuse attenuation coefficient for downwelling irradiance (K_d) at the beginning of the experiment. K_d was calculated by measuring changes in light intensities across the depth gradient using the cosine-corrected PAR sensor of a Diving-PAM (Walz), previously calibrated against a manufacturer-calibrated quantum sensor (LI-1400, LI-COR). The available light intensity at the depth of each transplant site, expressed as the percentage of incident light, was calculated based on the local K_d as $E_z = E_0\ e^{-K_d z}$ [6], where E_z is the % irradiance at z depth (in meters) and E_0 is the % irradiance at sea surface (100%). Variation in temperature and relative light levels throughout the duration of the experiment was recorded every 30 min from September 26 of 2014 until March 20 of 2015 by Onset HOBO data loggers (UA-002-64, Onset Computer Corporation) attached to the PVC panels (one logger per panel).

Photophysiology

To test how depth-dependent light variation affects the photosynthetic condition of corals' symbiotic algae, we measured the chlorophyll *a* (Chl *a*) fluorescence on coral fragments from the transplant experiment and on random colonies across the vertical distribution range of both species, using pulse amplitude modulated (PAM) fluorometry (Diving-PAM). Measurements were recorded on ten fragments (different genotypes) of each species at each depth before transplantation, and every two to three days during the week after transplantation. The effective quantum yield ($\Delta F/F_m$') of photosystem II (PSII) was recorded at noon during peak sunlight exposure, and the maximum quantum yield of PSII (F_v/F_m) at dusk. The maximum excitation pressure over PS II (Q_m) was calculated as $Q_m = 1 - [(\Delta F/F_m')/(F_v/F_m)]$[43]. $\Delta F/F_m$' was also recorded *in situ* on coral colonies of *O. annularis* ($n = 38$) and *O. franksi* ($n = 67$) randomly distributed over the full depth range of each species. In order to calculate Q_m on these colonies, we estimated F_v/F_m based on a linear regression with data obtained from a sub-sample of colonies

randomly distributed over the same depth range (n = 10 and n = 21 for *O. annularis* and *O. franksi*, respectively). Pearson's correlation coefficients revealed a strong positive correlation between F_v/F_m and depth in both *O. annularis* and *O. franksi* ($R^2 = 0.85$, $p < 0.01$ and $R^2 = 0.83$, $p < 0.01$), indicating a reliable prediction of F_v/F_m across depths. We used linear regression models to explore the relationship between Q_m and depth for *O. annularis* and *O. franksi* based on evidence that Q_m varies in a pattern that is roughly linear with depth in other coral species[43]. An Analysis of Covariance (ANCOVA) was conducted to test for differences in slopes and intercepts among regression models (interaction of species with depth). Due to technical issues with the Diving-PAM (loss in hermeticity), samples from the transplant experiment were transported from the transplant sites to the boat in a dark container to record measurements. During this short period of dark acclimation (<5 min), some components of the non-photochemical quenching could have relaxed[138], leading to a slight, yet nearly constant, underestimation of the $\Delta F/F_m$' recorded at noon and, as a result, of Q_m in all corals. Analyses were conducted using R version 3.6.1[139].

Microbiome

Small Subunit Ribosomal RNA (16S) amplicon library preparation and sequencing, sequence quality control and initial data processing

We quantified coral-associated microbiome communities in coral transplants to test if adaptive divergence between *O. annularis* and *O. franksi* is in part due to their microbial communities. Tissue samples were collected at the end of the transplant experiment using 1/8" metal corers by divers wearing Nitrile gloves and were immediately deposited in whirl pack bags. Once returned to the boat, each sample was gently washed with filter-sterile (0.2 µm) seawater, deposited in a sterile cryovial, and immediately preserved in liquid nitrogen. We extracted DNA from coral tissue samples using the MoBio Powersoil DNA Isolation Kit (MoBio Laboratories). Two-stage amplicon PCR was performed on the V4 region of the 16S small subunit prokaryotic rRNA gene[121,140]. Amplicons were barcoded with Fluidigm barcoded Illumina primers (8 cycles) and pooled in equal concentrations for sequencing. The amplicon pool was purified with AMPure XP beads and sequenced on the Illumina MiSeq sequencing platform at the DNA Services Facility at the University of Illinois at Chicago. Sequences were submitted to the National Center for Biotechnology Information (NCBI) Short Read Archive (SRA) under project number PRJNA717688.

Initial processing of 16S libraries was performed using the Quantitative Insights Into Microbial Ecology (QIIME; v1.9) package[141]. Primer sequences were trimmed, paired-end reads merged, and QIIME's default quality-control parameters were used to split libraries among samples. Chimeras were removed and 97%-similarity OTUs picked using USEARCH 7.0[142], QIIME's subsampled open-reference OTU-picking protocol[143], and the 97% GreenGenes 13_8 reference database[144]. Taxonomy was assigned using UCLUST and reads were aligned against the GreenGenes database using PyNAST[145]. FastTreeMP[146] was used to create a bacterial phylogeny with constraints defined by the GreenGenes reference phylogeny. OTUs classified as "unknown" (*i.e.*, sequences not classified at the kingdom level), chloroplast, mitochondria, or other potential contaminants were removed. Low coverage samples (< 223 useable reads) were omitted. Unless otherwise stated, downstream microbiome analyses and figure generation were performed in R version 3.2.5[139] using the phyloseq and ggplot2 packages[147,148].

ß-diversity group significance and differential abundance testing

To quantify differences among treatments, we used weighted UniFrac (wUniFrac) dissimilarity matrices using OTU-level relative abundances. Significant differences in bacterial assemblages were assessed by permutational multivariate analysis of variance (PERMANOVA) with wUniFrac distances and the explanatory variables host species and depth (*i.e.*, vegan::adonis)[149]. Both overall (*i.e.*, *O. annularis* and *O. franksi*) and species-specific models (*i.e.*, *O. annular*is or *O. franksi*) were tested. Heatmaps of OTU abundances were created using the phyloseq::plot_heatmap function[148]. Within-category microbiome variability (*i.e.*, wUniFrac distance) was calculated in QIIME using the make_distance_boxplots function, which also assesses significant differences in microbiome variability among categories via pairwise, nonparametric t-tests (1000 Monte Carlo permutations) with Bonferroni correction. To test for significant differences in OTU abundances across host species and depths, we employed negative binomial modelling using DESeq2[148,150]. Both the overall (*i.e.*, *O. annularis* and *O. franksi*) and species-specific models (*i.e.*, *O. annular*is or *O. franksi*) were tested. P-values for the significance of contrasts were generated based on Wald statistics, and false discovery rates were calculated using the Benjamini–Hochberg procedure.

Microalgal communities

Internal Transcribed Spacer 2 rRNA (ITS2) amplicon library preparation, sequencing, and initial processing

To quantify differences in dinoflagellate communities across species and depths, we used a two-stage amplicon PCR on the same DNA that was extracted and used for the 16S amplification. We amplified the Internal Transcribed Spacer 2 (ITS2) rRNA marker gene to characterize microalgal taxa within the family Symbiodiniaceae[108]. Once the PCR reactions were finished, samples were held at 4 °C before sequencing. Samples were sequenced using the Illumina MiniSeq platform at the DNA Services Facility at the University of Chicago, Illinois. Sequences were submitted to SymPortal for processing and quality checks[107]. Quality checking was performed using mothur[151], followed by taxonomic identification using blastn. The SymPortal pipeline then subdivides sequences into genus groupings and identified type profiles, referred to as defining intragenomic sequence variants (DIVs). Type profiles were only identified if a variant contained more than 200 sequences, and the sequences were subsequently named based on whether they had been used in the definition of the DIVs. The resulting absolute and relative count tables were imported into R version 3.5.2[139] for downstream analyses and figure generation using the phyloseq[148], vegan[149], microbiome[152], and ggplot2[147] packages.

ß-diversity group significance testing

To compare dinoflagellate communities across samples, we constructed Bray-Curtis and Jaccard dissimilarity matrices using absolute abundances. Significant differences in bacterial communities between sample types were assessed by PERMANOVA with Bray-Curtis and Jaccard distances and explanatory variables including host species, season, and depth using the adonis function from the vegan package[149]. We tested overall models that encompassed both species as well as species-specific models.

Results

Temperature and irradiance are higher and more variable in shallow environments

The K_d near the transplant sites was 0.40 m^{-1}, indicating that corals from the shallow (3.5 m) and deep (9.5 m) sites receive respectively ~25% and ~2% sea surface irradiance. Across the vertical distribution range of each species (Figure **3-1*a***), it is estimated that the light intensity varies between 18% and 62% sea surface irradiance for *O. annularis* and between 5% and 33% for *O. franksi*. Relative light levels recorded by data loggers indicated that the light exposure was nearly 5 times more variable in shallow water than in deep water. Daily temperatures were significantly higher in the shallow site (28.85 ± 0.96 ºC, mean ± s.d.) than in the deep site (28.46 ± 0.88 ºC; *t*-value = 3.92, $p < 0.001$; Figure **3-1*b***). However, based on the scaling quotient of temperature (Q_{10}) of *Orbicella* spp.[21], it is estimated that the metabolic rate variation due to differences in temperature among sites is negligible (~5%).

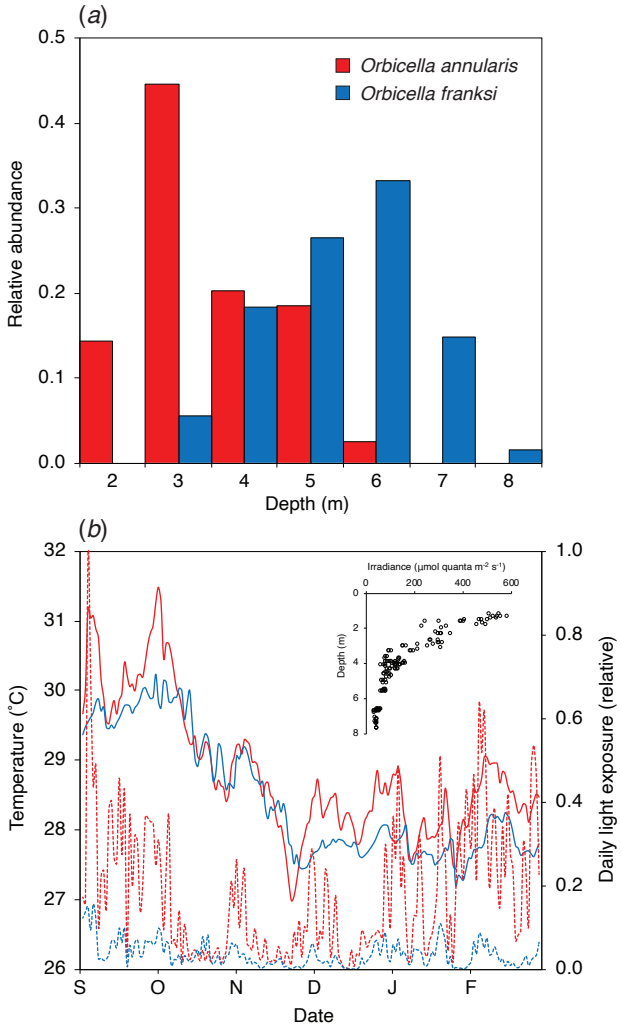

Figure **3-1**: (***a***) Vertical distribution of *O. annularis* and *O. franksi* around the transplant sites in Bocas del Toro, Panamá, previously established as part of the long-term monitoring of coral spawning in which nearly 500 *Orbicella* colonies were tagged and genotyped across the species depth range[16]. (***b***) Variation of the mean daily temperature (continuous lines) and relative light exposure (discontinuous lines) at the shallow (red) and deep (blue) transplant sites. The inset shows the light intensity variation across depths used to calculate the local K_d.

O. annularis experiences greater mortality in deep environments

Transplantation of *O. annularis* S-D (Δ_{depth} = 6 m) resulted in 26% mortality (Fisher exact test: p = 0.003) and was significantly higher than that of *O. franksi* colonies transplanted D-D (4% mortality, Fisher exact test: p = 0.04). *O. franksi* therefore has an advantage of 26% over *O.*

annularis in deep habitats. In contrast, *O. franksi* when transplanted D-S did remarkably well with only 2% mortality (Fisher exact test: $p = 0.63$). Mortality of the two species was not significantly different (0% mortality, Fisher exact test: $p = 0.60$), suggesting that *O. franksi* in shallow areas has no perceivable short-term (< six months) disadvantage relative to *O. annularis* (Fisher exact test: $p = 0.60$).

Photoacclimation of *O. annularis* is insufficient to compensate for reduced light

Symbionts of *O. annularis* exhibited a significant increase in F_v/F_m when transplanted S-D (0.622 ± 0.034) relative to corals transplanted S-S (0.541 ± 0.007) (*t*-value = -6.25, $p < 0.01$). On the contrary, symbionts of *O. franksi* transplanted D-S experienced a reduction in F_v/F_m (0.470 ± 0.052) relative to D-D transplants (0.630 ± 0.020; *t*-value = 0.55, $p < 0.01$). Transplantation of *O. annularis* S-D induced a significant reduction in Q_m (0.008 ± 0.076), relative to S-S transplantation (0.216 ± 0.163; *t*-value = 3.67, $p < 0.01$) (Figure **3-2*a*)**; while *O. franksi* exhibited a significant increase in Q_m (0.226 ± 0.156) when transplanted D-S, relative to D-D transplants (0.073 ± 0.056; *t*-value = 3.26, $p < 0.01$) (Figure **3-2*b***).

Estimations of Q_m on coral colonies along the vertical distribution of each species ranged from 0.099 to 0.673 in *O. annularis* and from 0.020 to 0.492 in *O. franksi* (Figure **3-2*c***). We found a significant species by depth interaction ($F_{(1,102)}=28.78$, $p<0.001$), indicating that the slope of the regression model describing the relationship between Q_m and depth was significantly different between species, being more than twice as pronounced in *O. annularis* (m=-0.13; $R^2=0.71$, $p<0.001$) than in *O. franksi* (m=-0.05; $R^2=0.50$, $p<0.001$). The linear regression of Q_m with depth indicated that the potential depth limit described by the bioenergetics of the coral-algae symbiosis (*i.e.*, where Q_m reaches the minimum theoretical value of 0) is 5.5. m for *O. annularis* and 7.8 m for *O. franksi* (Figure **3-2*c***), which nearly coincide with the observed lower limit of distribution of both species in the study area (Figure **3-1**).

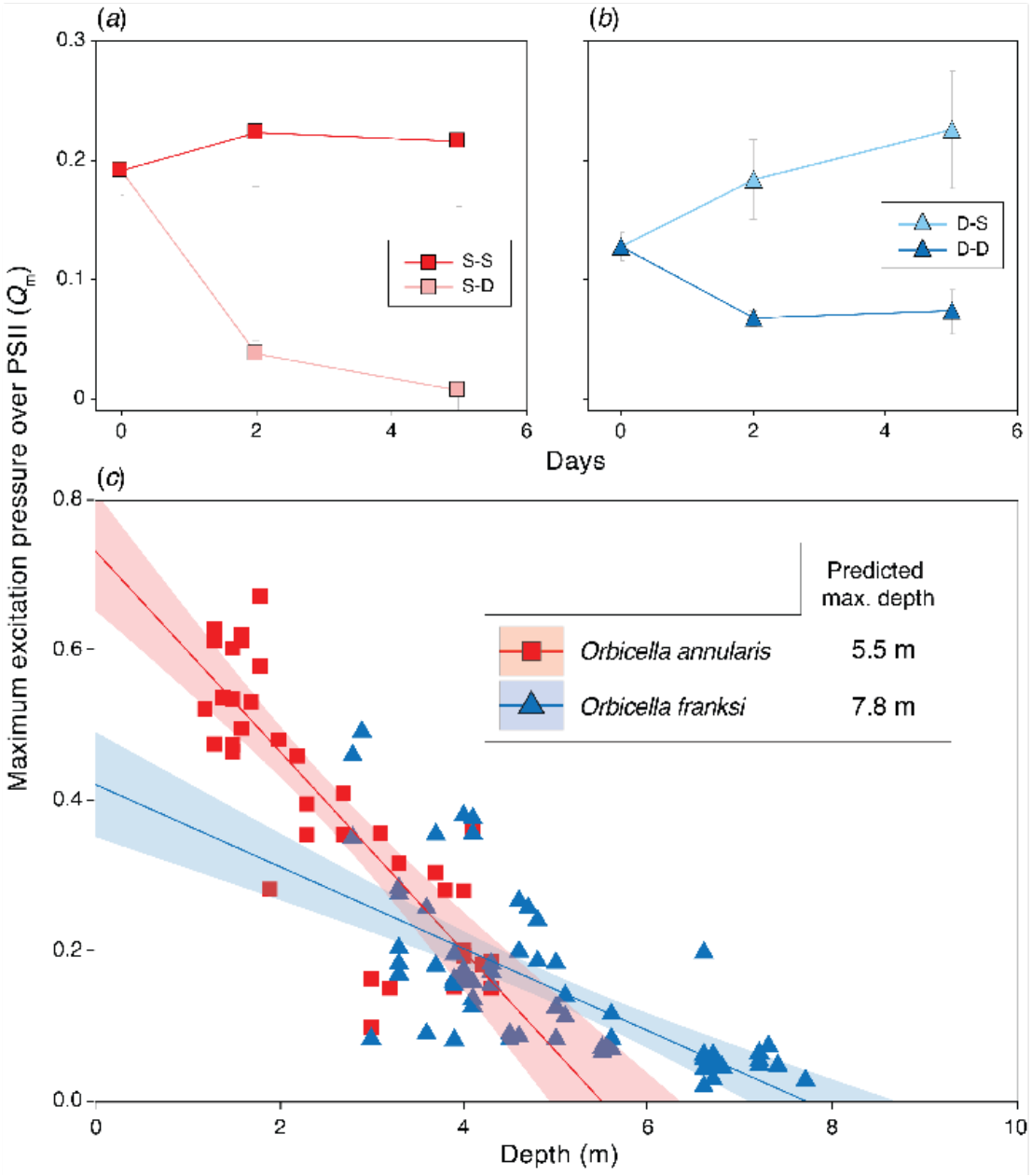

Figure **3-2**: Photoacclimation responses of *Orbicella* spp. across depths. Maximum excitation pressure over PS II (Q_m) is shown pre- and post-transplantation for *O. annularis* (***a***) and *O. franksi* (***b***). Values obtained in *O. annularis* transplanted S-S are shown in dark red while those transplanted S-D in pink. Values from *O. franksi* transplanted D-D are shown in dark blue while those transplanted D-S in light blue. (***c***) Q_m variation in *O. annularis* (red) and *O. franksi* (blue) along a depth gradient. A linear model was used to fit the data and predict the maximum potential depth limit described by Q_m for *O. annularis* [$Q_m = 0.735 - 0.133$*depth; $R^2 = 0.71$, $p < 0.001$] and *O. franksi* [$Q_m = 0.422 - 0.054$*depth; $R^2 = 0.50$, $p < 0.001$]. Clear lines represent 95% confidence intervals.

Changes in depth produces a major shift in *O. annularis* microbiome

After quality control, sequencing resulted in a total of 577,930 microbial reads (per sample median: 5,758; per sample mean: 9,173) partitioned across 14,274 unique OTUs. Overall, coral-associated prokaryote communities were significantly structured according to depth ($p = 0.001$), but not host species ($p = 0.12$) or depth by species interaction ($p = 0.86$; PERMANOVA on weighted UniFrac; Figure **3-3**). The change across depths is mainly driven by *O. annularis* ($p = 0.01$, Figure **3-3**). The strong response of *O. annularis* microbiomes to changes in depth can be visualized in differential patterns of OTU abundance among depths (Figure **3-3*a***).

Ten bacterial taxa were significantly enriched in shallow-water samples. OTUs enriched in shallow-water coral microbiomes are from the bacterial Orders Acidimicrobiales (1 OTU), Alteromonadales (1), Kiloniellales (2), Lactobacillales (1), Neisseriales (1), Oceanospirillales (3), and Synechococcales (1). The mean $\log_2$ fold change for enriched OTUs was 5.6.

Microbiome variability did not differ significantly between species with *O. annularis* (0.592 ± 0.008; mean UniFrac distance ± standard error) and *O. franksi* fragments (0.582 ± 0.008) ($p_{adj} = 0.358$). In contrast, microbiome variability differed significantly between depths, being greatest in *O. annularis* transplanted S-D (0.631 ± 0.013; mean UniFrac distance ± standard error) and significantly higher than *O. annularis* transplanted S-S (0.574 ± 0.008; $p_{adj} < 0.001$) or *O. franksi* transplanted D-S (0.580 ± 0.010; $p_{adj} = 0.006$) (Figure **3-3*b***). The larger microbiome variability in *O. annularis* transplanted deep is consistent with higher mortality and limited photoacclimation potential.

Symbiodiniaceae communities vary across species

Algal communities of *O. annularis* were significantly different from those of *O. franksi* regardless of the depth to which they were transplanted ($p < 0.05$; pairwise PERMANOVA on a Bray-Curtis matrix). Symbiodiniaceae genotypes belonging to the genera *Symbiodinium* (ITS2 type A3) and *Cladocopium* (C3an, C3an/C3, C7, and C7f) occurred in both coral species, although *Cladocopium* genotypes were more abundant in *O. franksi*. Genotypes from the genus *Breviolum* (B1 and B1/B1t) were detected in high abundance in *O. annularis,* and in many colonies from the shallow site (40% of them) were the only dominant symbiont. Only one *O. franksi* colony transplanted D-S hosted a *Breviolum* (B1) population. Genotypes belonging to the genus *Durusdinium* (D1, D1bl, D4, and D4c) were detected only in *O. franksi* transplanted D-D

(Figure **3-4**). Neither *O. annularis* nor *O. franksi* Symbiodiniaceae communities were significantly different when transplanted to a different depth ($p > 0.1$; pairwise PERMANOVA on a Bray-Curtis matrix).

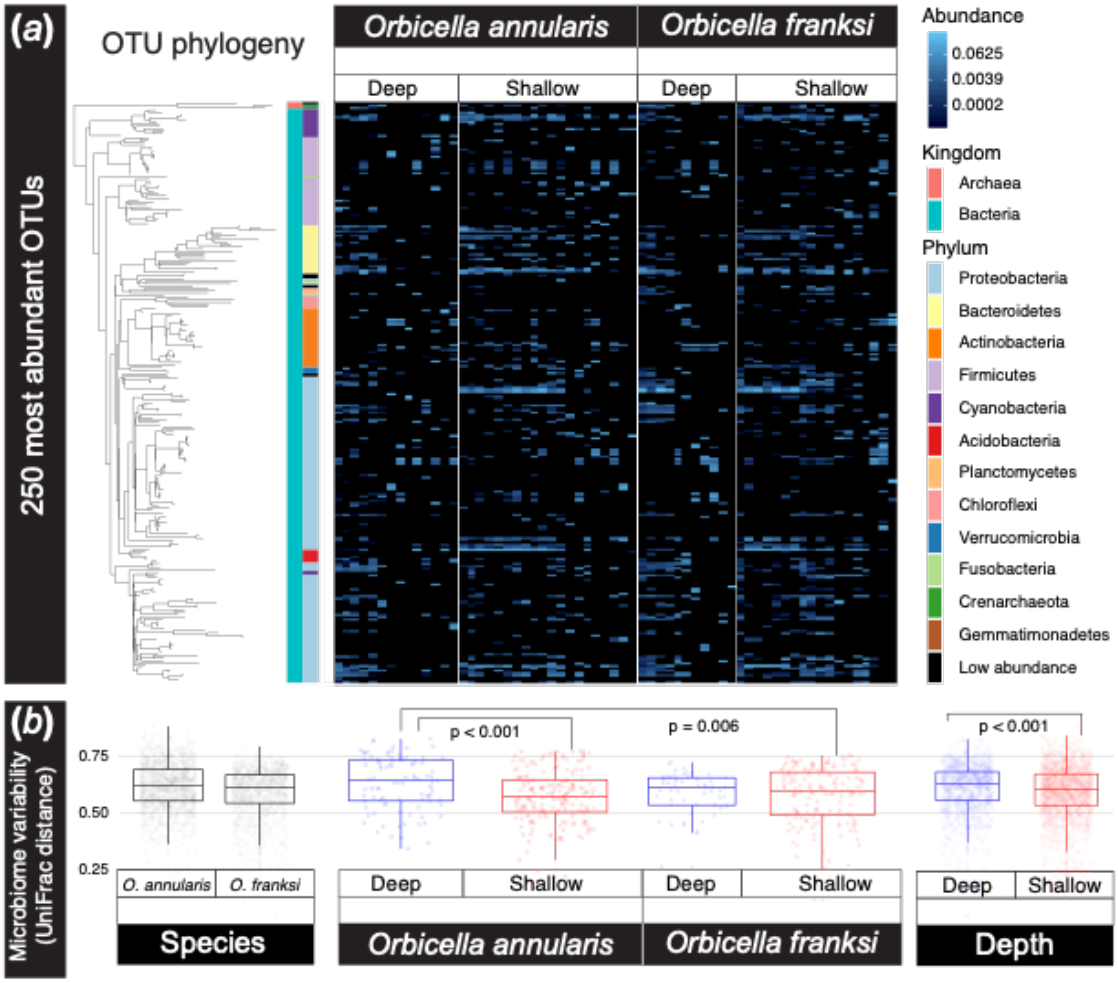

Figure **3-3**: *O. annularis* microbiomes vary across timepoints and depths while *O. franksi* communities remain consistent. (*a*) Relative abundances of the 250 most common OTUs reveal distinct patterns among *O. annularis* microbiomes at the two transplant depths while *O. franksi* abundance patterns remain largely consistent across treatments. Each column in the heatmap represents an individual microbiome sample and phylogenetic relationships among OTUs are shown on the left (FastTree maximum-likelihood tree). (*b*) Microbiome variability (*i.e.*, weighted UniFrac distances) was greatest in *O. annularis* corals transplanted to deep waters. Microbiome variability was higher in corals in deep waters than in shallow.

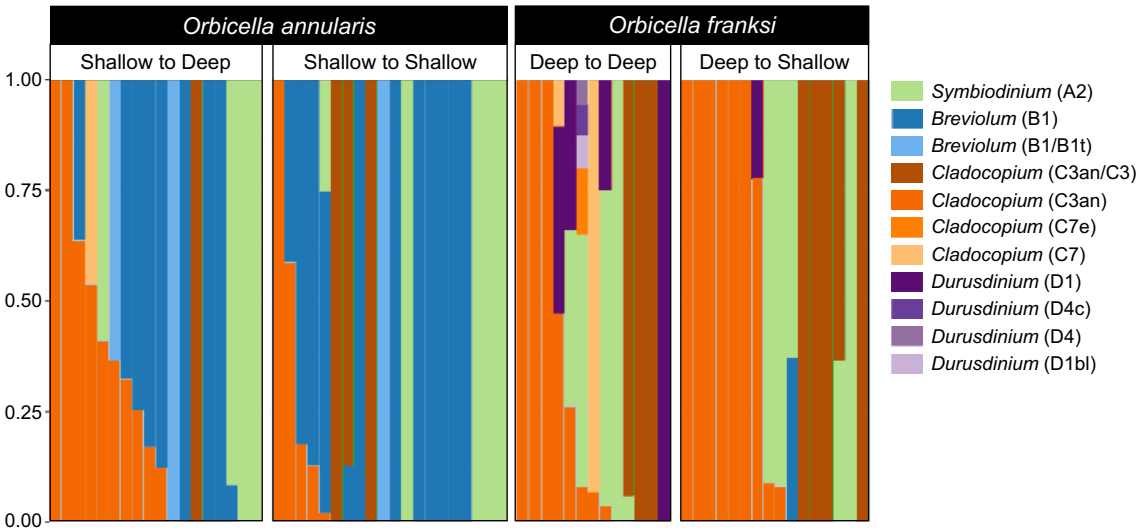

Figure **3-4**: Relative abundance bar plot of Symbiodiniaceae ITS2 profiles identified in *Orbicella* spp. by Symportal[107]. Variation in Symbiodiniaceae types is shown by species as well as by depth.

Discussion

Our study demonstrates that despite being genetically close[16], *O. annularis* and *O. franksi* have diverged physiologically and occupy distinct light environments in part due to the variation in their associated microbiotas (Symbiodiniaceae and bacterial communities). Following transplantation to deep habitats, *O. annularis* experiences a limited photoacclimation potential and disruption of the photosynthetic performance of its algal symbionts, consistent with increased mortality and significant microbiome community shifts with increased variability. By contrast, *O. franksi* maintained a robust physiological performance, a resilient microbiome composition with no significant community shifts or increased variability, and low mortality at both depths. Our study suggests that *O. annularis* is adapted to shallow environments characterized by a higher and more variable temperature and light regimes, while *O. franksi* is physiologically able to live in both shallow and deep habitats. The niches of these sibling species have diverged, and a large component of the niche separation seems to be related to variations in the photoacclimation capabilities and the microbial community of each species. The absence of *O. franksi* in shallow areas may be related to other ecological aspects not considered in our experiment, such as slow growth in an area of intense space competition, a restricted morphological plasticity for regulating

the light capture (see below) and/or disadvantages at the larval or recruitment stages in shallow waters.

The vertical distribution couples with the photoacclimation capabilities of each species

The vertical distribution of *O. annularis* and *O. franksi* is compressed toward shallower depths in Bocas del Toro compared to other clear-water sites in the Caribbean (*e.g.*, Curaçao[125] and Belize[14]). The vertical habitat compression in both species is consistent with the K_d measured in Bocas del Toro (0.40 m^{-1}), which is notably higher than in clear-water sites (0.06 m^{-1} in Curaçao and 0.08 m^{-1} in Belize[51,153]) and reflects the effect of the heavy rainfall patterns and runoff in the region on the optical properties of the water column[154]. This vertical habitat compression is consistent with other coral reefs exposed to water turbidity[10,100] and suggest that the light penetration into the water column associated with the local K_d is a determinant factor for the vertical zonation of *Orbicella* spp. Despite local differences in the vertical distribution ranges, *O. annularis* consistently occupies well-lit shallow areas of reefs where the potential for increased photosynthesis and calcification rates drives a steep competition for space with other corals. In contrast, *O. franksi* consistently dominates deeper reef areas characterized by low-light conditions and reduced coral-growth rates[155].

Our findings indicate that *O. annularis* experiences an almost complete loss of photosynthetic activity when transplanted deep. *O. annularis* fragments photoacclimate to low-light conditions by increasing the light energy conversion efficiency (*i.e*, increase in F_v/F_m)[45,46]. However, the extremely low values of Q_m reflect a trivial photosynthetic contribution of *O. annularis* symbionts to the host metabolism due to light-limited photosynthesis[43], suggesting that the photoacclimation potential is insufficient to compensate for the low-light conditions of deep environments. The higher mortality of *O. annularis* in the deep environment supports the insufficient autotrophic contribution to the host metabolism. Photoacclimation of *O. franksi* fragments transplanted to the shallow environment resulted in an increased fraction of photo-inactivated PSII reaction centers and capacity for thermal dissipation of excessive light energy absorbed[45,46]. But in contrast to *O. annularis*, the estimated Q_m in *O. franksi* do not indicate the occurrence of chronic photoinhibition in the shallow environment nor light-limitation in the deep environment, suggesting that *O. franksi* can maintain a more robust physiological performance across depths. The photoacclimation responses of both species in the transplant experiment were consistent with the rates of change in Q_m across their vertical distribution range, which collectively suggest that

the symbiotic algae of *O. annularis* are more sensitive to changes in light intensity with depth than symbionts of *O. franksi*.

Colony morphology can help modulate the light capture and photosynthetic energy acquisition along the vertical distribution range of corals[129,156]. The *Orbicella* species complex is unusual among other scleractinians in that they can simultaneously host multi-species communities of symbiotic dinoflagellates, whose composition follows environmental gradients of irradiance within colonies and across depths[17,19]. The dominance of *O. annularis* in shallow habitats correlates with its faster vertical growth among *Orbicella* species and with symbiotic partnerships with particular photoacclimation potential[13]. Its morphology (typically columnar) helps regulate the distribution of light energy for symbiotic algae across the colony surface, representing an advantageous strategy in high-light environments because it reduces the coral tissue area subjected to excessive irradiance[156]. When transplanted deep, this morphology may lead to acute light energy limitation which, in combination with the insufficient acclimation potential to compensate for low-light, can lead to negative energetic balances for the whole colony and eventual death. *O. franksi,* on the other hand, produce plate-like colonies to maximize light capture in deep environments. When transplanted to shallow well-lit environments, despite a potential for successful photoacclimation as indicated by our results, the plate-like morphology limits the capacity to regulate the internal light climate and allows very slow vertical growth. This slow growth makes *O. franksi* a poor competitor, likely explaining why this species is rare in shallow areas. Additionally, disadvantages at the larval or recruitment stage[157] may keep this species from being dominant in shallow waters. In fact, adaptation and strong selection across depths, may have promoted the evolution of habitat choice in these *Orbicella* species, as seems to happen in other anthozoans[158].

Another aspect that may influence the vertical distribution of *Orbicella* species is their heterotrophic feeding capacity. It has been indicated that corals from deep environments increase their metabolic reliance on heterotrophy to compensate for reduced photosynthesis[159,160]. The dominance of *O. franksi* in deep environments might be related to an increased heterotrophic feeding capacity relative to its sibling species. Unevenly distributed corallites that give the bumpy appearance to *O. franksi* colonies with larger coralites[13], may confer this species an advantage for passive suspension feeding[161]. However, results from previous studies indicate that colonies of *O. franksi* grow near the lowest growth potential determined by light availability in deep environments[162], suggesting that energy from heterotrophy may not be sufficient to maintain coral

growth. The typical plate-like morphology of this species instead of increasing the efficiency of passive suspension feeding, is an adaptation to maximize light capture in deep low-light habitats[11]. Overall, the evidence regarding the role of heterotrophy on the vertical distribution of *Orbicella* species is conflicting and inconclusive.

Host species drive symbiont communities

Species-specific associations with algal symbionts with contrasting photoacclimation capabilities may be a key axis of differentiation between *O. annularis* and *O. franksi.* Despite the higher and more variable temperature and light intensity in shallow areas, *Durusdinium trenchii* was not detected in *O. annularis* colonies. This symbiont is common among *Orbicella* and other coral species growing under harsh environmental conditions[17,18]. Surprisingly, this thermotolerant symbiont (ITS type D1/D1bl) was found in nearly 20% of *O. franksi* colonies from the deep environment. The increased abundance of *D. trenchii* in *O. franksi* may be related with the runoff impacts in the water column (*e.g.*, sedimentation and nutrient enrichment), a reduction in light penetration, and the mechanisms by which the coral-algae symbiosis interact with these environmental conditions[163]. The prevalence of *Breviolum* genotypes in *O. annularis* and *Cladocopium* genotypes in *O. franksi,* both in the shallow and deep transplant sites, is consistent with previous reports[122,163] and may indicate the formation of stable associations explained by the photoacclimative capabilities of dinoflagellates and the variability of physical factors within the vertical distribution range of each coral species[43,122]. The ITS2 analysis has a low resolution to differentiate linages within the same genus in symbiotic algal communities[164,165]. It is possible that complementary analysis with other molecular markers improves the phylogenetic resolution of Symbiodiniaceae (*i.e.,* species or population level), detecting differences in cryptic species/populations of *Cladocopium* spp. or *Breviolum* spp. uniquely associated with each *Orbicella* species like in other depth-segregated anthozoans (*e.g.,* the octocoral *Eunicea flexuosa* and scleractinians of the genus *Leptoseris* spp.)[158,166].

Microbiome communities vary across depths and are enriched in shallow habitats

Several Endozoicomonas OTUs were significantly enriched in shallow habitats. Endozoicimonaceae are diverse gammaproteobacterial symbionts of numerous marine hosts at varying depths and with a wide global distribution[167]. Members of this group are found in

abundance in the tissues of coral species and are considered to be true symbionts of corals which may provide a beneficial function[131,168]. Although their function within the coral host is not entirely clear, proposed benefits include nutrient acquisition, microbiome structuring and roles in coral health.

Members of the family Alteromonadaceae and the order Acidimicrobiales were also enriched in shallow areas. Alteromonadaceae belong to a diverse group of heterotrophic gammaproteobacteria known to associate with marine hosts and nutrient rich environments. Members of this group tolerate relatively high temperatures and have been used in coral probiotic studies as coral-associated bacteria capable of scavenging free radicals[169], and therefore could provide similar benefits in shallow, high-light environments. Similarly, Acidimicrobiales are known to be planktonic free-living photo-heterotrophs found in both temporal and tropical photic zones[170] and are associated with DOM in marine environments[171].

Finally, corals in shallow areas were also enriched for *Alloiococcus* and *Synechococcus*. *Alloiococcus* belongs to the group of gram-positive lactic acid bacteria, which are recognized for producing bacterial growth inhibitors that function to deter invading bacteria in their hosts[172]. *Synechococcus* is a photoautotrophic cyanobacterium found in surface waters harbouring abundant light. Both corals and their symbiotic algae are known to actively feed on *Synechococcus*[173,174] which is often found as a member of the coral surface mucus microbiome[134]. As a food for corals, it has been suggested that nitrogen-rich *Synechococcus* cells may increase bleaching recovery and coral health[175].

There is a continuing debate as to the relative role of coral host vs environment in shaping coral microbiomes. This study demonstrates that the responsiveness of coral microbiomes to environmental conditions differs significantly even among very closely related coral species. These differences in microbiome shifts may be related to the resilience of the coral host and its associated algal community to a particular habitat. Pantos et al.[131] found that environment is the major driver of microbiome structure in *Seriatopora hysterix*, not host genotype or Symbiodiniaceae strain. Our results do not contradict this finding but suggest that responsiveness to environmental conditions can differ significantly even among very closely related coral taxa.

Implications for coral reef conservation

A key finding in our study with implications for coral restoration is the increased mortality of *O. annularis* when transplanted to low-light environments. We suggest that to enhance survivorship during restoration, the particular light environment of source populations should be similar to the transplant sites. In this study, due to the high vertical attenuation of light (K_d = 0.40 m^{-1}), a 6 m increase in depth resulted in an order of magnitude reduction in irradiance and increased mortality of *O. annularis* by 26%. In a clear-water site (*e.g.*, K_d = 0.06 m^{-1}), this response would be expected to occur with an increase in depth of ~40 m. Giving the expensive nature of coral restoration, equating the light environment of donor and transplant sites will likely increase yield and decrease costs. Minimally, our approach can be used to estimate the maximum theoretical depth for each species in a given location with certain water optical quality, thereby providing guidance when choosing the location and depth for coral transplantation.

The second aspect of our findings is related to microbiome composition in different habitats across reefs. Our study suggests that the microbiome of shallow water specialists, like *O. annularis,* may be adapted to an environment with strong changes in light, temperature and salinity. A potential, and relatively unexplored, outcome from ongoing environmental change and disturbances on reef corals, is the instability of associated microbiomes across the vertical distribution range of species. Our study suggests that the microbiome of shallow-water species respond strongly to environmental change, with potential detrimental effects on the corals' survival. The instability in the coral microbiomes of shallow-water corals will potentially increase as a result of climate change, contributing to the ongoing coral decline in these reef areas[93,176].

Lastly, subtle differences in the water optical conditions can result in changes in the underwater light environment and the vertical distribution of coral species. Most coral reefs around the globe are currently threatened by the direct effects of sediments, pollutants and nutrients associated with coastal development and terrestrial runoff[84]. These conditions affect the water optical quality and, as a consequence, the light climate of corals and the survivorship of species at different depths. Although previous studies have suggested that deep-water species are more sensitive to changes in water optical conditions[51], our results suggest that at least some shallow-water specialists, like *O. annularis*, can be extremely vulnerable to these changes as their physiology/morphology is specialized for high light habitats. As the degradation of water optical properties in coral reefs continue, shallow-water specialists, which are typically major reef-building species, will likely become rare, shifting the structural and functional integrity of reefs.

Appendix

Data generated and analyzed in the productivity-biodiversity model

	Depth	Int. Irrad	Int. Prod	Int. Prod. Rel	PSII HT	Cs	PES	Empiric S	Predicted S	Residuals	R^2 model	p-val model	Pmax	Alpha	M	Delta	R	K_d	Authors	Location
1	2.5	40.10	0.44	100.00	2.05	87.86	12.14	146.23	149.36	-3.13	0.95	9.80E-06	11.31	0.043	22.81	-0.55	15.00	0.082	Roberts et al. (2019)	Papua New Guinea (Indo-Pacific)
2	7.5	26.61	0.42	96.12	2.56	70.19	25.94	169.71	165.28	4.43	0.95	9.80E-06	11.31	0.043	22.81	-0.55	15.00	0.082	Roberts et al. (2019)	Papua New Guinea (Indo-Pacific)
3	12.5	17.66	0.39	88.87	3.21	56.07	32.80	173.62	173.20	0.42	0.95	9.80E-06	11.31	0.043	22.81	-0.55	15.00	0.082	Roberts et al. (2019)	Papua New Guinea (Indo-Pacific)
4	17.5	11.72	0.34	77.05	4.02	44.79	32.26	169.50	172.57	-3.07	0.95	9.80E-06	11.31	0.043	22.81	-0.55	15.00	0.082	Roberts et al. (2019)	Papua New Guinea (Indo-Pacific)
5	22.5	7.78	0.27	61.47	5.03	35.78	25.69	164.40	165.00	-0.60	0.95	9.80E-06	11.31	0.043	22.81	-0.55	15.00	0.082	Roberts et al. (2019)	Papua New Guinea (Indo-Pacific)
6	27.5	5.16	0.20	45.43	6.30	28.59	16.85	154.00	154.79	-0.79	0.95	9.80E-06	11.31	0.043	22.81	-0.55	15.00	0.082	Roberts et al. (2019)	Papua New Guinea (Indo-Pacific)
7	32.5	3.43	0.14	31.87	7.88	22.84	9.03	148.00	145.78	2.22	0.95	9.80E-06	11.31	0.043	22.81	-0.55	15.00	0.082	Roberts et al. (2019)	Papua New Guinea (Indo-Pacific)
8	37.5	2.27	0.10	21.71	9.87	18.24	3.47	144.24	139.36	4.88	0.95	9.80E-06	11.31	0.043	22.81	-0.55	15.00	0.082	Roberts et al. (2019)	Papua New Guinea (Indo-Pacific)
9	42.5	1.51	0.06	14.58	12.35	14.57	0.01	131.00	135.37	-4.37	0.95	9.80E-06	11.31	0.043	22.81	-0.55	15.00	0.082	Roberts et al. (2019)	Papua New Guinea (Indo-Pacific)
10	5.0	36.46	0.35	100.00	1.89	95.42	4.58	6.50	6.83	-0.33	0.91	1.27E-02	9.19	0.028	24.99	-0.60	15.01	0.060	Huston (1985)	Jamaica (Caribbean)
11	10.0	27.01	0.33	95.75	2.26	79.70	16.05	12.00	10.90	1.10	0.91	1.27E-02	9.19	0.028	24.99	-0.60	15.01	0.060	Huston (1985)	Jamaica (Caribbean)
12	15.0	20.01	0.31	89.28	2.71	66.57	22.71	12.00	13.27	-1.27	0.91	1.27E-02	9.19	0.028	24.99	-0.60	15.01	0.060	Huston (1985)	Jamaica (Caribbean)
13	20.0	14.82	0.28	80.22	3.24	55.60	24.61	14.50	13.95	0.55	0.91	1.27E-02	9.19	0.028	24.99	-0.60	15.01	0.060	Huston (1985)	Jamaica (Caribbean)
14	30.0	8.14	0.20	56.64	4.64	38.79	17.85	11.50	11.54	-0.04	0.91	1.27E-02	9.19	0.028	24.99	-0.60	15.01	0.060	Huston (1985)	Jamaica (Caribbean)
15	3.0	42.75	0.20	100.00	1.88	99.73	0.27	14.60	15.63	-1.03	0.64	3.06E-02	5.00	0.060	20.00	-0.53	15.60	0.047	Loya (1972)	Gulf of Eilat (Indian Ocean)
16	5.0	38.91	0.20	100.00	1.97	94.88	5.11	19.58	16.84	2.74	0.64	3.06E-02	5.00	0.060	20.00	-0.53	15.60	0.047	Loya (1972)	Gulf of Eilat (Indian Ocean)
17	10.0	30.76	0.20	99.97	2.23	83.77	16.20	22.00	19.62	2.38	0.64	3.06E-02	5.00	0.060	20.00	-0.53	15.60	0.047	Loya (1972)	Gulf of Eilat (Indian Ocean)
18	15.0	24.32	0.20	99.86	2.53	73.96	25.90	15.22	22.05	-6.83	0.64	3.06E-02	5.00	0.060	20.00	-0.53	15.60	0.047	Loya (1972)	Gulf of Eilat (Indian Ocean)
19	20.0	19.23	0.20	99.54	2.87	65.30	34.24	24.33	24.14	0.19	0.64	3.06E-02	5.00	0.060	20.00	-0.53	15.60	0.047	Loya (1972)	Gulf of Eilat (Indian Ocean)
20	25.0	15.20	0.20	98.84	3.25	57.65	41.18	26.00	25.88	0.12	0.64	3.06E-02	5.00	0.060	20.00	-0.53	15.60	0.047	Loya (1972)	Gulf of Eilat (Indian Ocean)
21	30.0	12.02	0.19	97.56	3.68	50.90	46.66	29.67	27.25	2.42	0.64	3.06E-02	5.00	0.060	20.00	-0.53	15.60	0.047	Loya (1972)	Gulf of Eilat (Indian Ocean)
22	1.0	36.35	0.38	100.00	11.00	16.36	83.64	19.40	13.98	5.42	0.75	1.27E-03	9.75	0.060	40.00	-0.30	15.00	0.303	Chow et al. (2019)	Pulau Hantu (Indo-Pacific)
23	2.0	26.85	0.38	98.90	12.05	14.94	83.97	12.20	14.05	-1.85	0.75	1.27E-03	9.75	0.060	40.00	-0.30	15.00	0.303	Chow et al. (2019)	Pulau Hantu (Indo-Pacific)
24	3.0	19.83	0.37	96.72	13.20	13.64	83.09	11.80	13.86	-2.06	0.75	1.27E-03	9.75	0.060	40.00	-0.30	15.00	0.303	Chow et al. (2019)	Pulau Hantu (Indo-Pacific)
25	4.0	14.65	0.36	93.06	14.45	12.45	80.61	11.80	13.34	-1.54	0.75	1.27E-03	9.75	0.060	40.00	-0.30	15.00	0.303	Chow et al. (2019)	Pulau Hantu (Indo-Pacific)
26	5.0	10.82	0.34	87.38	15.83	11.37	76.01	11.20	12.37	-1.17	0.75	1.27E-03	9.75	0.060	40.00	-0.30	15.00	0.303	Chow et al. (2019)	Pulau Hantu (Indo-Pacific)
27	6.0	7.99	0.30	79.20	17.34	10.38	68.81	10.00	10.85	-0.85	0.75	1.27E-03	9.75	0.060	40.00	-0.30	15.00	0.303	Chow et al. (2019)	Pulau Hantu (Indo-Pacific)
28	7.0	5.90	0.26	68.66	18.98	9.48	59.18	9.60	8.82	0.78	0.75	1.27E-03	9.75	0.060	40.00	-0.30	15.00	0.303	Chow et al. (2019)	Pulau Hantu (Indo-Pacific)
29	8.0	4.36	0.22	56.84	20.79	8.66	48.19	10.20	6.50	3.70	0.75	1.27E-03	9.75	0.060	40.00	-0.30	15.00	0.303	Chow et al. (2019)	Pulau Hantu (Indo-Pacific)
30	9.0	3.22	0.17	45.24	22.77	7.91	37.33	3.00	4.22	-1.22	0.75	1.27E-03	9.75	0.060	40.00	-0.30	15.00	0.303	Chow et al. (2019)	Pulau Hantu (Indo-Pacific)
31	10.0	2.38	0.13	34.97	24.94	7.22	27.75	1.00	2.20	-1.20	0.75	1.27E-03	9.75	0.060	40.00	-0.30	15.00	0.303	Chow et al. (2019)	Pulau Hantu (Indo-Pacific)
32	1.0	37.24	0.26	100.00	5.50	32.75	67.25	19.75	20.30	-0.55	0.95	2.41E-06	6.45	0.060	26.58	-0.36	15.00	0.279	Chow et al. (2019)	Raffles Lighthouse (Indo-Pacific)
33	2.0	28.17	0.25	99.80	6.08	29.58	70.21	24.60	22.66	1.94	0.95	2.41E-06	6.45	0.060	26.58	-0.36	15.00	0.279	Chow et al. (2019)	Raffles Lighthouse (Indo-Pacific)
34	3.0	21.31	0.25	99.19	6.74	26.72	72.47	21.80	24.45	-2.65	0.95	2.41E-06	6.45	0.060	26.58	-0.36	15.00	0.279	Chow et al. (2019)	Raffles Lighthouse (Indo-Pacific)
35	4.0	16.12	0.25	97.87	7.46	24.14	73.73	27.60	25.46	2.14	0.95	2.41E-06	6.45	0.060	26.58	-0.36	15.00	0.279	Chow et al. (2019)	Raffles Lighthouse (Indo-Pacific)
36	5.0	12.20	0.24	95.54	8.25	21.81	73.73	24.60	25.46	-0.86	0.95	2.41E-06	6.45	0.060	26.58	-0.36	15.00	0.279	Chow et al. (2019)	Raffles Lighthouse (Indo-Pacific)
37	6.0	9.23	0.23	91.86	9.14	19.70	72.16	22.60	24.21	-1.61	0.95	2.41E-06	6.45	0.060	26.58	-0.36	15.00	0.279	Chow et al. (2019)	Raffles Lighthouse (Indo-Pacific)
38	7.0	6.98	0.22	86.40	10.11	17.80	68.60	24.20	21.38	2.82	0.95	2.41E-06	6.45	0.060	26.58	-0.36	15.00	0.279	Chow et al. (2019)	Raffles Lighthouse (Indo-Pacific)
39	8.0	5.28	0.20	78.80	11.20	16.08	62.73	15.40	16.70	-1.30	0.95	2.41E-06	6.45	0.060	26.58	-0.36	15.00	0.279	Chow et al. (2019)	Raffles Lighthouse (Indo-Pacific)
40	9.0	4.00	0.18	69.21	12.39	14.52	54.68	10.20	10.30	-0.10	0.95	2.41E-06	6.45	0.060	26.58	-0.36	15.00	0.279	Chow et al. (2019)	Raffles Lighthouse (Indo-Pacific)
41	10.0	3.02	0.15	58.44	13.72	13.12	45.32	3.00	2.85	0.15	0.95	2.41E-06	6.45	0.060	26.58	-0.36	15.00	0.279	Chow et al. (2019)	Raffles Lighthouse (Indo-Pacific)

	Depth	Int. Irrad	Int. Prod	Int. Prod. Rel	PSII HT	Cs	PES	Empiric S	Predicted S	Residuals	R^2 model	p-val model	Pmax	Alpha	M	Delta	R	K_d	Authors	Location
42	1.1	46.19	0.40	100.00	2.16	84.61	15.39	4.60	12.28	-7.68	0.80	1.65E-05	10.24	0.044	21.56	-0.51	15.22	0.060	Sheppard (1980)	Chagos Seaward (Indian-Ocean)
43	2.2	43.13	0.40	99.75	2.23	81.72	18.02	7.79	14.47	-6.68	0.80	1.65E-05	10.24	0.044	21.56	-0.51	15.22	0.060	Sheppard (1980)	Chagos Seaward (Indian-Ocean)
44	3.2	40.70	0.40	99.50	2.30	79.35	20.15	19.83	16.23	3.60	0.80	1.65E-05	10.24	0.044	21.56	-0.51	15.22	0.060	Sheppard (1980)	Chagos Seaward (Indian-Ocean)
45	5.8	34.73	0.40	98.61	2.49	73.23	25.38	24.62	20.57	4.05	0.80	1.65E-05	10.24	0.044	21.56	-0.51	15.22	0.060	Sheppard (1980)	Chagos Seaward (Indian-Ocean)
46	9.0	28.70	0.39	97.09	2.75	66.48	30.61	30.12	24.91	5.21	0.80	1.65E-05	10.24	0.044	21.56	-0.51	15.22	0.060	Sheppard (1980)	Chagos Seaward (Indian-Ocean)
47	12.0	23.99	0.38	95.13	3.01	60.70	34.43	33.31	28.08	5.23	0.80	1.65E-05	10.24	0.044	21.56	-0.51	15.22	0.060	Sheppard (1980)	Chagos Seaward (Indian-Ocean)
48	18.9	15.88	0.35	88.07	3.71	49.26	38.81	34.57	31.71	2.86	0.80	1.65E-05	10.24	0.044	21.56	-0.51	15.22	0.060	Sheppard (1980)	Chagos Seaward (Indian-Ocean)
49	24.1	11.63	0.32	79.72	4.34	42.06	37.66	28.92	30.76	-1.84	0.80	1.65E-05	10.24	0.044	21.56	-0.51	15.22	0.060	Sheppard (1980)	Chagos Seaward (Indian-Ocean)
50	29.8	8.24	0.27	67.64	5.17	35.33	32.31	20.44	26.32	-5.88	0.80	1.65E-05	10.24	0.044	21.56	-0.51	15.22	0.060	Sheppard (1980)	Chagos Seaward (Indian-Ocean)
51	36.0	5.66	0.21	52.88	6.25	29.21	23.67	14.80	19.15	-4.35	0.80	1.65E-05	10.24	0.044	21.56	-0.51	15.22	0.060	Sheppard (1980)	Chagos Seaward (Indian-Ocean)
52	41.7	4.04	0.16	40.41	7.42	24.61	15.79	10.57	12.61	-2.04	0.80	1.65E-05	10.24	0.044	21.56	-0.51	15.22	0.060	Sheppard (1980)	Chagos Seaward (Indian-Ocean)
53	44.9	3.34	0.14	34.22	8.17	22.35	11.88	8.80	9.36	-0.56	0.80	1.65E-05	10.24	0.044	21.56	-0.51	15.22	0.060	Sheppard (1980)	Chagos Seaward (Indian-Ocean)
54	47.8	2.79	0.12	29.08	8.95	20.40	8.68	8.28	6.71	1.57	0.80	1.65E-05	10.24	0.044	21.56	-0.51	15.22	0.060	Sheppard (1980)	Chagos Seaward (Indian-Ocean)
55	60.9	1.28	0.06	13.73	13.30	13.73	0.00	6.02	-0.49	6.51	0.80	1.65E-05	10.24	0.044	21.56	-0.51	15.22	0.060	Sheppard (1980)	Chagos Seaward (Indian-Ocean)
56	1.5	45.12	0.43	100.00	1.80	99.84	0.16	5.19	10.46	-5.27	0.85	4.31E-04	11.05	0.043	24.03	-0.57	15.00	0.060	Sheppard (1980)	Chagos Lagoon (Indian Ocean)
57	3.7	39.45	0.43	99.30	1.95	92.44	6.86	18.09	14.88	3.21	0.85	4.31E-04	11.05	0.043	24.03	-0.57	15.00	0.060	Sheppard (1980)	Chagos Lagoon (Indian Ocean)
58	6.5	33.37	0.42	98.10	2.14	83.98	14.12	21.12	19.67	1.45	0.85	4.31E-04	11.05	0.043	24.03	-0.57	15.00	0.060	Sheppard (1980)	Chagos Lagoon (Indian Ocean)
59	9.5	27.79	0.42	96.30	2.38	75.62	20.68	24.40	24.01	0.39	0.85	4.31E-04	11.05	0.043	24.03	-0.57	15.00	0.060	Sheppard (1980)	Chagos Lagoon (Indian Ocean)
60	12.1	23.79	0.41	94.30	2.60	69.17	25.13	26.92	26.94	-0.02	0.85	4.31E-04	11.05	0.043	24.03	-0.57	15.00	0.060	Sheppard (1980)	Chagos Lagoon (Indian Ocean)
61	17.5	17.28	0.38	88.47	3.13	57.59	30.88	32.48	30.74	1.74	0.85	4.31E-04	11.05	0.043	24.03	-0.57	15.00	0.060	Sheppard (1980)	Chagos Lagoon (Indian Ocean)
62	24.5	11.34	0.33	76.56	3.98	45.25	31.31	26.88	31.02	-4.14	0.85	4.31E-04	11.05	0.043	24.03	-0.57	15.00	0.060	Sheppard (1980)	Chagos Lagoon (Indian Ocean)
63	30.3	8.01	0.27	63.62	4.85	37.08	26.54	26.99	27.87	-0.88	0.85	4.31E-04	11.05	0.043	24.03	-0.57	15.00	0.060	Sheppard (1980)	Chagos Lagoon (Indian Ocean)
64	40.4	4.37	0.17	40.43	6.88	26.18	14.25	23.29	19.76	3.53	0.85	4.31E-04	11.05	0.043	24.03	-0.57	15.00	0.060	Sheppard (1980)	Chagos Lagoon (Indian Ocean)

Depth: depth intervals (in m), Int. Irrad: estimated daily integrated irradiance (mol quanta m^{-2} d^{-1}), Int. Prod: estimated daily integrated productivity (mol O_2 m^{-2} d^{-1}), Int. Prod. Rel: daily integrated productivity (relative to maximum), PSII HT: PSII half-time under available irradiance at depth z (h), Cs: Energy expenditure in photorepair by the symbiotic algae (relative), PES: photosynthetic energy supply to coral hosts (relative), Empiric S: coral species richness reported in each study at each depth, Predicted S: coral richness predicted by the model, Residuals: fitting deviation, R^2 model: explanatory power of the model, p-val model: statistical significance, Pmax: estimated maximum photosynthesis (µmol O_2 m^{-2} s^{-1}), Alpha: Slope of linear increase in photosynthesis at subsaturating irradiance (µmol O_2 µmol quanta $^{-1}$), M: Maximum PSII half-time when the available irradiance tends to 0, Delta: Rate of change of PSII half-time with respect to the available irradiance, R: relative costs of repair the photosynthetic apparatus, K_d: light attenuation coefficient.

REFERENCES

1 Muscatine, L. & Porter, J. W. Reef corals: mutualistic symbioses adapted to nutrient-poor environments. *BioScience* **27**, 454-460, doi:10.2307/1297526 (1977).

2 Enríquez, S., Méndez, E. R., Hoegh-Guldberg, O. & Iglesias-Prieto, R. Key functional role of the optical properties of coral skeletons in coral ecology and evolution. *Proc. R. Soc. B.* **284**, 20161667, doi:10.1098/rspb.2016.1667 (2017).

3 Goreau, T. F. & Goreau, N. I. The physiology of skeleton formation in corals. II. Calcium deposition by hermatypic corals under various conditions in the reef. *Biol. Bull.* **117**, 239-250, doi:10.2307/1538903 (1959).

4 Colombo-Pallotta, M. F., Rodríguez-Román, A. & Iglesias-Prieto, R. Calcification in bleached and unbleached *Montastraea faveolata*: evaluating the role of oxygen and glycerol. *Coral Reefs* **29**, 899-907 (2010).

5 Perry, C. T., Spencer, T. & Kench, P. S. Carbonate budgets and reef production states: a geomorphic perspective on the ecological phase-shift concept. *Coral Reefs* **27**, 853-866 (2008).

6 Kirk, J. T. O. *Light and photosynthesis in aquatic ecosystems*. Third edn, (Cambridge University Press, 2011).

7 Stoddart, D. R. Ecology and morphology of recent coral reefs. *Biol. Rev.* **44**, 433-498, doi:DOI 10.1111/j.1469-185X.1969.tb00609.x (1969).

8 Lesser, M. P., Slattery, M. & Leichter, J. J. Ecology of mesophotic coral reefs. *J. Exp. Mar. Biol. Ecol.* **375**, 1-8 (2009).

9 Roberts, T. E. *et al.* Testing biodiversity theory using species richness of reef-building corals across a depth gradient. *Biol. Lett.* **15**, 20190493, doi:doi:10.1098/rsbl.2019.0493 (2019).

10 López-Londoño, T. *et al.* Physiological and ecological consequences of the water optical properties degradation on reef corals. *Coral Reefs* **40**, 1243-1256, doi:10.1007/s00338-021-02133-7 (2021).

11 Kahng, S. E. *et al.* Community ecology of mesophotic coral reef ecosystems. *Coral Reefs* **29**, 255-275, doi:10.1007/s00338-010-0593-6 (2010).

12 Maritorena, S. & Guillocheau, N. Optical properties of water and spectral light absorption by living and non-living particles and by yellow substances in coral reef waters of French Polynesia. *Mar. Ecol. Prog. Ser.* **131**, 245-255, doi:DOI 10.3354/meps131245 (1996).

13 Weil, E. & Knowlton, N. A multi-character analysis of the Caribbean coral *Montastraea annularis* (Ellis and Solander, 1786) and its two sibling species, *M. faveolata* (Ellis and Solander, 1786) and *M. franksi* (Gregory, 1895). *Bull. Mar. Sci.* **55**, 151-175 (1994).

14 Pandolfi, J. M. & Budd, A. F. Morphology and ecological zonation of Caribbean reef corals: the *Montastraea 'annularis'* species complex. *Mar. Ecol. Prog. Ser.* **369**, 89-102 (2008).

15 Fukami, H. *et al.* Geographical differences in species boundaries among members of the *Montastraea annularis* complex based on molecular and morphological markers. *Evolution* **58**, 324-337 (2004).

16 Levitan, D., Fogarty, N., Jara, J., Lotterhos, K. & Knowlton, N. Genetic, spatial, and temporal components to precise spawning synchrony in reef building corals of the *Montastraea annularis* species complex. *Evolution* **65**, 1254–1270 (2011).

17 Rowan, R., Knowlton, N., Baker, A. & Jara, J. Landscape ecology of algal symbionts creates variation in episodes of coral bleaching. *Nature* **388**, 265-269, doi:Doi 10.1038/40843 (1997).

18 LaJeunesse, T. C., Smith, R. T., Finney, J. & Oxenford, H. Outbreak and persistence of opportunistic symbiotic dinoflagellates during the 2005 Caribbean mass coral bleaching event. *Proc. R. Soc. B.* **276**, 4139-4148, doi:doi:10.1098/rspb.2009.1405 (2009).

19 Kemp, D. W. *et al.* Spatially distinct and regionally endemic *Symbiodinium* assemblages in the threatened Caribbean reef-building coral *Orbicella faveolata*. *Coral Reefs* **34**, 535-547, doi:10.1007/s00338-015-1277-z (2015).

20 Warner, M. E., LaJeunesse, T. C., Robison, J. D. & Thur, R. M. The ecological distribution and comparative photobiology of symbiotic dinoflagellates from reef corals in Belize: potential implications for coral bleaching. *Limnol. Oceanogr.* **51**, 1887-1897, doi:DOI 10.4319/lo.2006.51.4.1887 (2006).

21 Scheufen, T., Kramer, W. E., Iglesias-Prieto, R. & Enriquez, S. Seasonal variation modulates coral sensibility to heat-stress and explains annual changes in coral productivity. *Sci. Rep.* **7**, 4937, doi:10.1038/s41598-017-04927-8 (2017).

22 Prada, C. *et al.* Linking photoacclimation responses and microbiome shifts between depth-segregated sibling species of reef corals. *bioRxiv*, doi:DOI: 10.1101/2021.10.18.464812 (2021).

23 Connell, J. H. Diversity in tropical rain forests and coral reefs. High diversity of trees and corals is maintained only in a nonequilibrium state. *Science* **199**, 1302-1310, doi:DOI 10.1126/science.199.4335.1302 (1978).

24 Hughes, T. P. Community structure and diversity of coral reefs: the role of history. *Ecology* **70**, 275-279, doi:10.2307/1938434 (1989).

25 Cornell, H. V. & Karlson, R. H. Coral species richness: ecological versus biogeographical influences. *Coral reefs* **19**, 37-49 (2000).

26 Fraser, R. H. & Currie, D. J. The species richness-energy hypothesis in a system where historical factors are thought to prevail: coral reefs. *Am. Nat.* **148**, 138-159 (1996).

27 Wright, D. H. Species-energy theory: an extension of species-area theory. *Oikos* **41**, 496-506 (1983).

28 Rosenzweig, M. L. & Abramsky, Z. in *Species diversity in ecological communities. Historical and geographical perspectives* (eds R. E. Ricklefs & D. Schluter) Ch. 5, 52-65 (The University of Chicago Press, 1993).

29 Cusens, J., Wright, S. D., McBride, P. D. & Gillman, L. N. What is the form of the productivity–animal-species-richness relationship? A critical review and meta-analysis. *Ecology* **93**, 2241-2252, doi:https://doi.org/10.1890/11-1861.1 (2012).

30 Long, S. P., Humphries, S. & Falkowski, P. G. Photoinhibition of photosynthesis in nature. *Annu. Rev. Plant Physial. Plant Mol. BioI.* **45**, 633-662, doi:DOI 10.1146/annurev.pp.45.060194.003221 (1994).

31 Maurer, B. A. *Untangling ecological complexity: the macroscopic perspective*. (University of Chicago Press, 1999).

32 Gotelli, N. J. *et al.* Patterns and causes of species richness: a general simulation model for macroecology. *Ecol. Lett.* **12**, 873-886 (2009).

33 Abrams, P. A. Monotonic or unimodal diversity-productivity gradients: what does competition theory predict? *Ecology* **76**, 2019-2027 (1995).

34 Fukami, T. & Morin, P. J. Productivity–biodiversity relationships depend on the history of community assembly. *Nature* **424**, 423-426, doi:10.1038/nature01785 (2003).

35 Huston, M. A. Disturbance, productivity, and species diversity: empiricism vs. logic in ecological theory. *Ecology* **95**, 2382-2396 (2014).

36 Duncan, C., Thompson, J. R. & Pettorelli, N. The quest for a mechanistic understanding of biodiversity-ecosystem services relationships. *Proc. R. Soc. B.* **282**, 20151348, doi:doi:10.1098/rspb.2015.1348 (2015).

37 Frankowiak, K. *et al.* Photosymbiosis and the expansion of shallow-water corals. *Sci. Adv.* **2**, e1601122, doi:10.1126/sciadv.1601122 (2016).

38 Huner, N. P. A., Öuist, G. & Sarhan, F. Energy balance and acclimation to light and cold. *Trends Plant Sci.* **3**, 224-230 (1998).

39 Iglesias-Prieto, R. & Trench, R. K. Acclimation and adaptation to irradiance in symbiotic dinoflagellates .1. Responses of the photosynthetic unit to changes in photon flux-density. *Mar. Ecol. Prog. Ser.* **113**, 163-175, doi:DOI 10.3354/meps113163 (1994).

40 Iglesias-Prieto, R. & Trench, R. K. Photoadaptation, photoacclimation and niche diversification in invertebrate-dinoflagellate symbioses. *Proc. 8th Int. Coral Reef Sym.* **2**, 1319-1324 (1997).

41 Roth, M. S. The engine of the reef: photobiology of the coral–algal symbiosis. *Front. Microbiol.* **5**, 1-22, doi:10.3389/fmicb.2014.00422 (2014).

42 Muscatine, L., McCloskey, L. R. & Marian, R. E. Estimating the daily contribution of carbon from zooxanthellae to coral animal respiration. *Limnol. Oceanogr.* **26**, 601-611, doi:https://doi.org/10.4319/lo.1981.26.4.0601 (1981).

43 Iglesias-Prieto, R., Beltrán, V. H., LaJeunesse, T. C., Reyes-Bonilla, H. & Thomé, P. E. Different algal symbionts explain the vertical distribution of dominant reef corals in the eastern Pacific. *Proc. R. Soc. Lond. B* **271**, 1757-1763, doi:10.1098/rspb.2004.2757 (2004).

44 Enríquez, S., Merino, M. & Iglesias-Prieto, R. Variations in the photosynthetic performance along the leaves of the tropical seagrass Thalassia testudinum. *Mar. Biol.* **140**, 891-900, doi:10.1007/s00227-001-0760-y (2002).

45 Hoegh-Guldberg, O. & Jones, R. J. Photoinhibition and photoprotection in symbiotic dinoflagellates from reef-building corals. *Mar. Ecol. Prog. Ser.* **183**, 73-86, doi:DOI 10.3354/meps183073 (1999).

46 Gorbunov, M. Y., Kolber, Z. S., Lesser, M. P. & Falkowski, P. G. Photosynthesis and photoprotection in symbiotic corals. *Limnol. Oceanogr.* **46**, 75-85, doi:DOI 10.4319/lo.2001.46.1.0075 (2001).

47 Warner, M. E., Lesser, M. P. & Ralph, P. J. in *Chlorophyll a Fluorescence in Aquatic Sciences: Methods and Applications* Ch. Chapter 10, 209-222 (2010).

48 Jørgensen, S. E. & Bendoricchio, G. *Fundamentals of ecological modelling*. Third edn, Vol. 21 (Elsevier Sceince B. V., 2001).

49 Ackleson, S. G. Light in shallow waters: A brief research review. *Limnol. Oceanogr.* **48**, 323-328, doi:DOI 10.4319/lo.2003.48.1_part_2.0323 (2003).

50 Anthony, K. R. N., Ridd, P. V., Orpin, A. R., Larcombe, P. & Lough, J. Temporal variation of light availability in coastal benthic habitats: effects of clouds, turbidity, and tides. *Limnol. Oceanogr.* **49**, 2201-2211, doi:DOI 10.4319/lo.2004.49.6.2201 (2004).

51 Vermeij, M. J. A. & Bak, R. P. M. How are coral populations structured by light? Marine light regimes and the distribution of *Madracis*. *Mar. Ecol. Prog. Ser.* **233**, 105-116, doi:DOI 10.3354/meps233105 (2002).

52 Hennige, S. J. *et al.* Acclimation and adaptation of scleractinian coral communities along environmental gradients within an Indonesian reef system. *J. Exp. Mar. Biol. Ecol.* **391**, 143-152, doi:10.1016/j.jembe.2010.06.019 (2010).

53 Scheufen, T., Iglesias-Prieto, R. & Enríquez, S. Changes in the number of symbionts and Symbiodinium cell pigmentation modulate differentially coral light absorption and

photosynthetic performance. *Front Mar Sci* **4**, 309, doi:10.3389/fmars.2017.00309 (2017).

54 Jassby, A. D. & Platt, T. Mathematical formulation of the relationship between photosynthesis and light for phytoplankton. *Limnol. Oceanogr.* **21**, 540-547 (1976).

55 Veron, J. E. N. *Corals in space and time. The biogeography and evolution of the Scleractinia*. 321 (Cornell University Press, 1995).

56 Stehli, F. G. & Wells, J. W. Diversity and age patterns in hermatypic corals. *Syst. Zool.* **20**, 115-126 (1971).

57 Huston, M. A. Patterns of species diversity in relation to depth at Discovery Bay, Jamaica. *Bull. Mar. Sci.* **37**, 928-935 (1985).

58 Loya, Y. Community structure and species diversity of hermatypic corals at Eilat, Red Sea. *Mar. Biol.* **13**, 100-123, doi:10.1007/BF00366561 (1972).

59 Sheppard, C. R. C. Coral cover, zonation and diversity on reef slopes of Chagos Atolls, and population structures of the major species. *Mar. Ecol. Prog. Ser.* **2**, 193-205 (1980).

60 Chow, G. S. E., Chan, Y. K. S., Jain, S. S. & Huang, D. Light limitation selects for depth generalists in urbanised reef coral communities. *Mar. Environ. Res.* **147**, 101-112, doi:10.1016/j.marenvres.2019.04.010 (2019).

61 Nelder, J. A. & Mead, R. A Simplex Method for Function Minimization. *J. Comput.* **7**, 308-313, doi:10.1093/comjnl/7.4.308 (1965).

62 R: A languate and environment for statistical computing. Retrieved from http://www.R-project.org (R Foundation for Statistical Computing, Vienna, Austria, 2010).

63 Brown, B. E. *et al.* Diurnal changes in photochemical efficiency and xanthophyll concentrations in shallow water reef corals: evidence for photoinhibition and photoprotection. *Coral Reefs* **18**, 99-105 (1999).

64 Lesser, M. P. & Gorbunov, M. Y. Diurnal and bathymetric changes in chlorophyll fluorescence yields of reef corals measured in situ with a fast repetition rate fluorometer. *Mar. Ecol. Prog. Ser.* **212**, 69-77, doi:DOI 10.3354/meps212069 (2001).

65 Hill, R. & Ralph, P. J. Diel and seasonal changes in fluorescence rise kinetics of three scleractinian corals. *Funct. Plant Biol.* **32**, 549-559 (2005).

66 Anthony, K. R. N. & Hoegh-Guldberg, O. Variation in coral photosynthesis, respiration and growth characteristics in contrasting light microhabitats: an analogue to plants in forest gaps and understoreys? *Funct. Ecol.* **17**, 246-259, doi:DOI 10.1046/j.1365-2435.2003.00731.x (2003).

67 Fabricius, K. E. & De'ath, G. Photosynthetic symbionts and energy supply determine octocoral biodiversity in coral reefs. *Ecology* **89**, 3163-3173 (2008).

68 Jokiel, P. L. Solar ultraviolet radiation and coral reef epifauna. *Science* **207**, 1069-1071 (1980).

69 Ben-Zvi, O., Eyal, G. & Loya, Y. Response of fluorescence morphs of the mesophotic coral *Euphyllia paradivisa* to ultra-violet radiation. *Sci. Rep.* **9**, 5245, doi:10.1038/s41598-019-41710-3 (2019).

70 Todd, P. A. Morphological plasticity in scleractinian corals. *Biol. Rev.* **83**, 315-337, doi:10.1111/j.1469-185x.2008.00045.x (2008).

71 Kaniewska, P., Anthony, K., Sampayo, E., Campbell, P. & Hoegh-Guldberg, O. Implications of geometric plasticity for maximizing photosynthesis in branching corals. *Mar. Biol.* **161**, 313-328 (2014).

72 Lesser, M. P., Stochaj, W. R., Tapley, D. W. & Shick, J. M. Bleaching in coral reef anthozoans: effects of irradiance, ultraviolet radiation, and temperature on the activities of protective enzymes against active oxygen. *Coral Reefs* **8**, 225-232, doi:10.1007/BF00265015 (1990).

73 Skirving, W. *et al.* Remote sensing of coral bleaching using temperature and light: progress towards an operational algorithm. *Remote Sens.* **10**, 18 (2018).

74 Fisher, R., Bessell-Browne, P. & Jones, R. Synergistic and antagonistic impacts of suspended sediments and thermal stress on corals. *Nat. Comm.* **10**, 2346 (2019).

75 Gonzalez-Espinosa, P. C. & Donner, S. D. Cloudiness reduces the bleaching response of coral reefs exposed to heat stress. *Glob. Change Biol.* **00**, 1-13, doi:https://doi.org/10.1111/gcb.15676 (2021).

76 Cacciapaglia, C. & van Woesik, R. Climate-change refugia: shading reef corals by turbidity. *Glob. Change Biol.* **22**, 1145-1154, doi:https://doi.org/10.1111/gcb.13166 (2016).

77 Prada, C. & Hellberg, M. E. Speciation-by-depth on coral reefs: sympatric divergence with gene flow or cryptic transient isolation? *J. Evol. Biol.* **34**, 128-137, doi:https://doi.org/10.1111/jeb.13731 (2021).

78 Rippe, J. P., Dixon, G., Fuller, Z. L., Liao, Y. & Matz, M. Environmental specialization and cryptic genetic divergence in two massive coral species from the Florida Keys Reef Tract. *Mol. Ecol.* **30**, 3468-3484, doi:https://doi.org/10.1111/mec.15931 (2021).

79 Anthony, K. R. N. & Fabricius, K. E. Shifting roles of heterotrophy and autotrophy in coral energetics under varying turbidity. *J. Exp. Mar. Biol. Ecol.* **252**, 221-253 (2000).

80 Hoogenboom, M., Rodolfo-Metalpa, R. & Ferrier-Pagès, C. Co-variation between autotrophy and heterotrophy in the Mediterranean coral *Cladocora caespitosa*. *J. Exp. Biol.* **213**, 2399-2409 (2010).

81 Conti-Jerpe, I. E. *et al.* Trophic strategy and bleaching resistance in reef-building corals. *Sci. Adv.* **6**, eaaz5443, doi:10.1126/sciadv.aaz5443 (2020).

82 Houlbrèque, F. & Ferrier-Pagès, C. Heterotrophy in tropical scleractinian corals. *Biol. Rev.* **84**, 1-17, doi:https://doi.org/10.1111/j.1469-185X.2008.00058.x (2009).

83 Kramer, N., Tamir, R., Eyal, G. & Loya, Y. Coral morphology portrays the spatial distribution and population size-structure along a 5–100 m depth gradient. *Front Mar Sci* **7**, doi:10.3389/fmars.2020.00615 (2020).

84 Carlson, R. R., Foo, S. A. & Asner, G. P. Land use impacts on coral reef health: a ridge-to-reef perspective. *Front Mar Sci* **6**, 562, doi:10.3389/fmars.2019.00562 (2019).

85 Burke, L., Reytar, K., Spalding, M. & Perry, A. *Reefs at risk revisited*. (World Resources Institute, 2011).

86 Odum, H. T. & Odum, E. P. Trophic Structure and Productivity of a Windward Coral Reef Community on Eniwetok Atoll. *Ecol. Monogr.* **25**, 291-320 (1955).

87 Wilkinson, C. *Status of coral reefs of the world: 2008*. (Global Coral Reef Monitoring Network and Reef and Rainforest Research Centre, Townsville, 2008).

88 Lough, J. M., Anderson, K. D. & Hughes, T. P. Increasing thermal stress for tropical coral reefs: 1871–2017. *Sci. Rep.* **8**, 6079, doi:10.1038/s41598-018-24530-9 (2018).

89 Bruno, J. F. & Selig, E. R. Regional decline of coral cover in the Indo-Pacific: timing, extent, and subregional comparisons. *PLoS One* **2**, e711, doi:10.1371/journal.pone.0000711 (2007).

90 Jackson, J., Donovan, M., Cramer, K. & Lam, V. *Status and trends of Caribbean coral reefs: 1970-2012*. (Global Coral Reef Monitoring Network, IUCN, 2014).

91 Zaneveld, J. R. *et al.* Overfishing and nutrient pollution interact with temperature to disrupt coral reefs down to microbial scales. *Nat. Commun.* **7**, 11833 (2016).

92 Hoegh-Guldberg, O. *et al.* Coral reefs under rapid climate change and ocean acidification. *Science* **318**, 1737-1742 (2007).

93 Hughes, T. P. *et al.* Global warming transforms coral reef assemblages. *Nature* **556**, 492-496 (2018).

94 Shantz, A. A. & Burkepile, D. E. Context-dependent effects of nutrient loading on the coral-algal mutualism. *Ecology* **95**, 1995-2005, doi:Doi 10.1890/13-1407.1 (2014).

95 Morris, L. A., Voolstra, C. R., Quigley, K. M., Bourne, D. G. & Bay, L. K. Nutrient availability and metabolism affect the stability of coral–Symbiodiniaceae symbioses. *Trends Microbiol.* **27**, 678-689, doi:https://doi.org/10.1016/j.tim.2019.03.004 (2019).

96 Junjie, R. K., Browne, N. K., Erftemeijer, P. L. A. & Todd, P. A. Impacts of sediments on coral energetics: partitioning the effects of turbidity and settling particles. *PLoS ONE* **9**, e107195 (2014).

97 Pollock, F. J. *et al.* Sediment and turbidity associated with offshore dredging increase coral disease prevalence on nearby reefs. *PLoS ONE* **9**, e102498 (2014).

98 Bessell-Browne, P., Negri, A. P., Fisher, R., Clode, P. L. & Jones, R. Impacts of light limitation on corals and crustose coralline algae. *Sci. Rep.* **7**, 11553 (2017).

99 Omachi, C. Y. *et al.* Light availability for reef-building organisms in a plume-influenced shelf. *Cont. Shelf Res.* **181**, 25-33, doi:https://doi.org/10.1016/j.csr.2019.05.005 (2019).

100 Morgan, K. M., Moynihan, M. A., Sanwlani, N. & Switzer, A. D. Light limitation and depth-variable sedimentation drives vertical reef compression on turbid coral reefs. *Front Mar Sci* **7**, 931 (2020).

101 Pizarro, V. *et al.* Unraveling the structure and composition of Varadero Reef, an improbable and imperiled coral reef in the Colombian Caribbean. *Peerj* **5**, e4119 (2017).

102 Mogollón, J. V. *El Canal del Dique. Historia de un desastre ambiental*. (El Ancora Editores, Bogotá, 2013).

103 Restrepo, J. D., Escobar, R. & Tosic, M. Fluvial fluxes from the Magdalena River into Cartagena Bay, Caribbean Colombia: Trends, future scenarios, and connections with upstream human impacts. *Geomorphology* **302**, 92-105, doi:http://dx.doi.org/10.1016/j.geomorph.2016.11.007 (2018).

104 Lonin, S., Parra, C., Andrade, C. & Thomas, Y. Patrones de la pluma turbia del canal del Dique en la bahía de Cartagena. *Bol. Cient. CIOH* **22**, 77-89 (2004).

105 SORCE/SIM. *SOlar Radiation and Climate Experiment, Spectral Irradiance Monitor SIM*, <https://lasp.colorado.edu/home/sorce/data/> (2020).

106 Stat, M., Pochon, X., Cowie, R. O. M. & Gates, R. D. Specificity in communities of Symbiodinium in corals from Johnston Atoll. *Mar. Ecol. Prog. Ser.* **386**, 83-96 (2009).

107 Hume, B. C. C. *et al.* SymPortal: a novel analytical framework and platform for coral algal symbiont next-generation sequencing ITS2 profiling. *Mol. Ecol. Resour.* **19**, 1063-1080, doi:10.1111/1755-0998.13004 (2019).

108 LaJeunesse, T. C. *et al.* Systematic revision of Symbiodiniaceae highlights the antiquity and diversity of coral endosymbionts. *Curr. Biol.* **28**, 2570-2580.e2576, doi:https://doi.org/10.1016/j.cub.2018.07.008 (2018).

109 Jeffrey, S. W. & Humphrey, G. F. New spectrophotometric equations for determining chlorophylls a, b, c1 and c2 in higher-plants, algae and natural phytoplankton. *Biochem. Physiol. Pflanz.* **167**, 191-194 (1975).

110 Enríquez, S., Méndez, E. R. & Iglesias-Prieto, R. Multiple scattering on coral skeletons enhances light absorption by symbiotic algae. *Limnol. Oceanogr.* **50**, 1025-1032, doi:DOI 10.4319/lo.2005.50.4.1025 (2005).

111 Vásquez-Elizondo, R. M. *et al.* Absorptance determinations on multicellular tissues. *Photosynth. Res.* **132**, 311-324, doi:10.1007/s11120-017-0395-6 (2017).

112 Marsh, J. A. Primary productivity of reef-building calcareous red algae. *Ecology* **51**, 255-263, doi:10.2307/1933661 (1970).

113 Lang, J. C. Status of coral reefs in the western Atlantic: results of initial surveys, Atlantic and Gulf Rapid Reef Assessment (AGRAA) Program. *Atoll Res. Bull.* **496**, 625 (2003).

114 Chalker, B. E. Simulating light-saturation curves for photosynthesis and calcification by reef-building corals. *Mar. Biol.* **63**, 135-141, doi:10.1007/bf00406821 (1981).

115 Holcomb, M., Tambutte, E., Allemand, D. & Tambutte, S. Light enhanced calcification in Stylophora pistillata: effects of glucose, glycerol and oxygen. *Peerj* **2**, e375 (2014).

116 DiPerna, S., Hoogenboom, M., Noonan, S. & Fabricius, K. Effects of variability in daily light integrals on the photophysiology of the corals *Pachyseris speciosa* and *Acropora millepora*. *PLoS One* **13**, e0203882, doi:10.1371/journal.pone.0203882 (2018).

117 Wyman, K. D., Dubinsky, Z., Porter, J. W. & Falkowski, P. G. Light-absorption and utilization among hermatypic corals: a study in Jamaica, West-Indies. *Mar. Biol.* **96**, 283-292, doi:Doi 10.1007/Bf00427028 (1987).

118 Rodríguez-Román, A., Hernández-Pech, X., Thomé, P. E., Enríquez, S. & Iglesias-Prieto, R. Photosynthesis and light utilization in the Caribbean coral *Montastraea faveolata* recovering from a bleaching event. *Limnol. Oceanogr.* **51**, 2702-2710 (2006).

119 Hill, J. F. & Govindjee. The controversy over the minimum quantum requirement for oxygen evolution. *Photosynth. Res.* **122**, 97-112, doi:10.1007/s11120-014-0014-8 (2014).

120 Tosic, M., Restrepo, J. D., Lonin, S., Izquierdo, A. & Martins, F. Water and sediment quality in Cartagena Bay, Colombia: seasonal variability and potential impacts of pollution. *Estuar. Coast. Shelf Sci.* **216**, 187-203 (2019).

121 Roitman, S. *et al.* Surviving marginalized reefs: assessing the implications of the microbiome on coral physiology and survivorship. *Coral Reefs* **39**, 795-807, doi:10.1007/s00338-020-01951-5 (2020).

122 LaJeunesse, T. Diversity and community structure of symbiotic dinoflagellates from Caribbean coral reefs. *Mar. Biol.* **141**, 387-400, doi:10.1007/s00227-002-0829-2 (2002).

123 Thornhill, D. J., Lewis, A. M., Wham, D. C. & LaJeunesse, T. C. Host-specialist lineages dominate the adaptive radiation of reef coral endosymbionts. *Evolution* **68**, 352-367 (2014).

124 Smith, E. G. *et al.* Low Symbiodiniaceae diversity in a turbid marginal reef environment. *Coral Reefs* **39**, 545-553, doi:10.1007/s00338-020-01956-0 (2020).

125 Van Veghel, M. L. J. *Polymorphism in the Caribbean reef building coral Montastrea annularis. Ph.D. thesis*, University of Amsterdam, (1994).

126 Kennedy, E. V. *et al.* Avoiding coral reef functional collapse requires local and global action. *Curr. Biol.* **23**, 912-918 (2013).

127 Thompson, J. R., Rivera, H. E., Closek, C. J. & Medina, M. Microbes in the coral holobiont: partners through evolution, development, and ecological interactions. *Front. Cell. Infect. Microbiol.* **4**, 1-20 (2015).

128 Gilbert, S. F. *et al.* Symbiosis as a source of selectable epigenetic variation: taking the heat for the big guy. *Phil. Trans. R. Soc. B.* **365**, 671-678, doi:10.1098/rstb.2009.0245 (2010).

129 Hoogenboom, M. O., Connolly, S. R. & Anthony, K. R. N. Interactions between morphological and physiological plasticity optimize energy acquisition in corals. *Ecology* **89**, 1144-1154, doi:Doi 10.1890/07-1272.1 (2008).

130 Rohwer, F., Seguritan, V., Azam, F. & Knowlton, N. Diversity and distribution of coral-associated bacteria. *Mar. Ecol. Prog. Ser.* **243**, 1-10 (2002).

131 Pantos, O., Bongaerts, P., Dennis, P. G., Tyson, G. W. & Hoegh-Guldberg, O. Habitat-specific environmental conditions primarily control the microbiomes of the coral *Seriatopora hystrix*. *ISME J.* **9**, 1916-1927, doi:10.1038/ismej.2015.3 (2015).

132 Kellogg, C. A. *et al.* Comparing bacterial community composition between healthy and white plague-like disease states in *Orbicella annularis* using PhyloChip™ G3 microarrays. *PLos ONE* **8**, e79801, doi:10.1371/journal.pone.0079801 (2013).

133 Peixoto, R. S., Rosado, P. M., Leite, D. C. d. A., Rosado, A. S. & Bourne, D. G. Beneficial microorganisms for corals (BMC): proposed mechanisms for coral health and resilience. *Front. Microbiol.* **8**, 341 (2017).
134 Marchioro, G. M. *et al.* Microbiome dynamics in the tissue and mucus of acroporid corals differ in relation to host and environmental parameters. *Peerj* **8**, e9644 (2020).
135 Egan, K. E. *et al.* Predicting the distribution of threatened orbicellid corals in shallow and mesophotic reef ecosystems. *Mar. Ecol. Prog. Ser.* **667**, 61-81 (2021).
136 Pandolfi, J. M., Lovelock, C. E. & Budd, A. F. Character release following extinction in a Caribbean reef coral species complex. *Evolution* **56**, 479-501 (2002).
137 Hereford, J. A quantitative survey of local adaptation and fitness trade-offs. *Am. Nat.* **173**, 579-588 (2009).
138 Ralph, P. & Gademann, R. Rapid Light Curves: a powerful tool to assess photosynthetic activity. *Aquat. Bot.* **82**, 222-237, doi:10.1016/j.aquabot.2005.02.006 (2005).
139 R: A language and environment for statistical computing (R Foundation for Statistical Computing, Vienna, Austria, 2015).
140 Apprill, A., McNally, S., Parsons, R. & Webe, L. Minor revision to V4 region SSU rRNA 806R gene primer greatly increases detection of SAR11 bacterioplankton. *Aquat. Microb. Ecol.* **75**, 129–137 (2015).
141 Caporaso, J. G. *et al.* QIIME allows analysis of high-throughput community sequencing data. *Nat. Methods* **7**, 335-336 (2010).
142 Edgar, R. C. Search and clustering orders of magnitude faster than BLAST. *Bioinformatics* **26**, 2460-2461, doi:10.1093/bioinformatics/btq461 (2010).
143 Rideout, J. R. *et al.* Subsampled open-reference clustering creates consistent, comprehensive OTU definitions and scales to billions of sequences. *Peerj* **2**, e545 (2014).
144 McDonald, D. *et al.* An improved Greengenes taxonomy with explicit ranks for ecological and evolutionary analyses of bacteria and archaea. *ISME J.* **6**, 610-618 (2012).
145 Caporaso, J. G. *et al.* PyNAST: a flexible tool for aligning sequences to a template alignment. *Bioinformatics* **26**, 266-267 (2010).
146 Price, M. N., Dehal, P. S. & Arkin, A. P. FastTree 2–approximately maximum-likelihood trees for large alignments. *PLoS ONE* **5**, e9490 (2010).
147 Wickham, H. *ggplot2: elegant graphics for data analysis*. (Springer, 2009).
148 McMurdie, P. J. & Holmes, S. phyloseq: an R package for reproducible interactive analysis and graphics of microbiome census data. *PLos ONE* **8**, e61217, doi:10.1371/journal.pone.0061217 (2013).
149 vegan: Community Ecology Package v. 2.4-3 (2017).
150 Love, M. I., Huber, W. & Anders, S. Moderated estimation of fold change and dispersion for RNA-seq data with DESeq2. *Genome Biol.* **15**, 550 (2014).
151 Schloss, P. D. *et al.* Introducing mothur: open-source, platform-independent, community-supported software for describing and comparing microbial communities. *Appl. Environ. Microbiol.* **75**, 7537-7541, doi:10.1128/aem.01541-09 (2009).
152 microbiome R package. Tools for microbiome analysis in R. (2017).
153 Banaszak, A., Lesser, M., Kuffner, I. & Ondrusek, M. Relationship between ultraviolet (UV) radiation and mycosporine-like amino acids (MAAS) in marine organisms. *Bull. Mar. Sci.* **63**, 617-628 (1998).
154 Kaufmann, K. W. & Thompson, R. C. Water temperature variation and the meteorological and hydrographic environment of Bocas del Toro, Panama. *Caribb. J. Sci.* **41**, 392-413 (2005).

155 Cohen, I. & Dubinsky, Z. Long term photoacclimation responses of the coral *Stylophora pistillata* to reciprocal deep to shallow transplantation: photosynthesis and calcification. *Front Mar Sci* **2**, 45, doi:10.3389/fmars.2015.00045 (2015).

156 Kaniewska, P. *et al.* Importance of macro- versus microstructure in modulating light levels inside coral colonies. *J. Phycol.* **47**, 846-860, doi:https://doi.org/10.1111/j.1529-8817.2011.01021.x (2011).

157 Baird, A. H., Babcock, R. C. & Mundy, C. P. Habitat selection by larvae influences the depth distribution of six common coral species. *Mar. Ecol. Prog. Ser.* **252**, 289-293 (2003).

158 Prada, C. *et al.* Cryptic diversity hides host and habitat specialization in a gorgonian-algal symbiosis. *Mol. Ecol.* **23**, 3330-3340, doi:https://doi.org/10.1111/mec.12808 (2014).

159 Ferrier-Pagès, C. *et al.* Symbiotic stony and soft corals: Is their host-algae relationship really mutualistic at lower mesophotic reefs? *Limnol. Oceanogr.* (2021).

160 Lesser, M. P. *et al.* Photoacclimatization by the coral *Montastraea cavernosa* in the mesophotic zone: light, food, and genetics. *Ecology* **91**, 990-1003, doi:Doi 10.1890/09-0313.1 (2010).

161 Porter, J. W. Autotrophy, heterotrophy, and resource partitioning in Caribbean reef-building corals. *Am. Nat.* **110**, 731-742 (1976).

162 Groves, S. H. *et al.* Growth rates of *Porites astreoides* and *Orbicella franksi* in mesophotic habitats surrounding St. Thomas, US Virgin Islands. *Coral Reefs* **37**, 345-354, doi:10.1007/s00338-018-1660-7 (2018).

163 Garren, M., Walsh, S. M., Caccone, A. & Knowlton, N. Patterns of association between *Symbiodinium* and members of the *Montastraea annularis* species complex on spatial scales ranging from within colonies to between geographic regions. *Coral Reefs* **25**, 503-512, doi:10.1007/s00338-006-0146-1 (2006).

164 LaJeunesse, T. C. & Thornhill, D. J. Improved resolution of reef-coral endosymbiont (*Symbiodinium*) species diversity, ecology, and evolution through psbA non-coding region genotyping. *PLos ONE* **6**, e29013, doi:10.1371/journal.pone.0029013 (2011).

165 Stat, M. *et al.* Variation in *Symbiodinium* ITS2 sequence assemblages among coral colonies. *PLos ONE* **6**, e15854, doi:10.1371/journal.pone.0015854 (2011).

166 Pochon, X. *et al.* Depth specialization in mesophotic corals (*Leptoseris* spp.) and associated algal symbionts in Hawai'i. *R. Soc. Open Sci.* **2**, 140351, doi:doi:10.1098/rsos.140351 (2015).

167 Neave, M. J., Apprill, A., Ferrier-Pagès, C. & Voolstra, C. R. Diversity and function of prevalent symbiotic marine bacteria in the genus *Endozoicomonas*. *Appl. Microbiol. Biotechnol.* **100**, 8315-8324, doi:10.1007/s00253-016-7777-0 (2016).

168 Bayer, T. *et al.* The microbiome of the Red Sea coral *Stylophora pistillata* is dominated by tissue-associated *Endozoicomonas* bacteria. *Appl. Environ. Microbiol.* **79**, 4759-4762, doi:10.1128/aem.00695-13 (2013).

169 Dungan, A. M., Bulach, D., Lin, H., van Oppen, M. J. & Blackall, L. L. Development of a free radical scavenging bacterial consortium to mitigate oxidative stress in cnidarians. *MMicrob. Biotechnol.* **14**, 2025-2040, doi:doi:10.1111/1751-7915.13877 (2021).

170 Angly, F. E. *et al.* Marine microbial communities of the Great Barrier Reef lagoon are influenced by riverine floodwaters and seasonal weather events. *Peerj* **4**, e1511 (2016).

171 Osterholz, H., Kirchman, D. L., Niggemann, J. & Dittmar, T. Diversity of bacterial communities and dissolved organic matter in a temperate estuary. *FEMS Microbiol. Ecol.* **94**, fiy119 (2018).

172 Ringø, E. *et al.* Lactic acid bacteria in finfish—An update. *Front. Microbiol.* **9**, 1818 (2018).

173 Jeong, H. J. *et al.* Heterotrophic feeding as a newly identified survival strategy of the dinoflagellate *Symbiodinium*. *Proc. Natl. Acad. Sci. U.S.A.* **109**, 12604-12609 (2012).
174 McNally, S. P., Parsons, R. J., Santoro, A. E. & Apprill, A. Multifaceted impacts of the stony coral *Porites astreoides* on picoplankton abundance and community composition. *Limnol. Oceanogr.* **62**, 217-234, doi:https://doi.org/10.1002/lno.10389 (2017).
175 Meunier, V. *et al.* Bleaching forces coral's heterotrophy on diazotrophs and *Synechococcus*. *ISME J.* **13**, 2882-2886 (2019).
176 Bridge, T. C. *et al.* Depth-dependent mortality of reef corals following a severe bleaching event: implications for thermal refuges and population recovery. *F1000Research* **2** (2013).

VITA

Tomás López-Londoño

EDUCATION

2022 Ph.D. Biology, Pennsylvania State University, University Park PA, USA
2015 M.Sc. Marine Sciences (*Cum Laude*), Universidad Nacional Autónoma de México, Puerto Morelos, Mexico
2007 B.Sc. Marine Biology, Universidad Jorge Tadeo Lozano, Bogotá, Colombia

SELECTED PUBLICATIONS

López-Londoño T., *et al*. 2022. Photosynthetic energy supply drives biodiversity patterns in reef corals. *In review: Nature*.
López-Londoño T., *et al*. 2022. Robustness vs specialization: physiological strategies leading to niche partitioning driven by light availability in reef corals. *In prep*.
López-Londoño T., *et al*. 2022. Light gradients as an axis for species diversification and niche partitioning in symbiotic corals. *In prep*.
Gómez-Campo K., **T. López-Londoño**, *et al.* 2022. Energy (cost)-based calcification modelling resolves climate change uncertainties in coral reefs. *In prep*.
Prada C. & **T. López-Londoño**, *et al*. 2022. Linking photoacclimation responses and microbiome shifts between depth-segregated sibling species of reef corals. *In press: Royal Society Open Science.*
López-Londoño T., *et al*. 2021. Physiological and ecological consequences of the water optical properties degradation on reef corals. *Coral Reefs* 40:1243–1256
González-Guerrero L., ... **T. López-Londoño**, *et al*. 2021. Validation of parameters and protocols derived from chlorophyll *a* fluorescence commonly utilised in marine ecophysiological studies. *Functional Plant Biology:* FP21101
Roitman S, **T. López-Londoño**, *et al*. 2020. Surviving marginalized reefs: assessing the implications of the microbiome on coral physiology and survivorship. *Coral Reefs* 39: 795–807.

PROFESSIONAL DEVELOPMENT

2014 *Internship*. Medina Lab. Pennsylvania State University, University Park PA, USA
2007-13 *Research Assistant*. Instituto de Investigaciones Marinas y Costeras INVEMAR, National Monitoring System of Coral Reefs in Colombia SIMAC / Integrated National Adaptation Project INAP. Santa Marta, Colombia

TEACHING EXPERIENCE (PENNSYLVANIA STATE UNIVERSITY)

Population and Communities (BIOL220W). Lab Teaching Assistant SP/17, FA/18, FA/19, FA/20, FA/21
Basic Concepts and Biodiversity (BIOL110W). Lab Teaching Assistant SP/22

GRANTS AND HONORS

2021 Penn State Biology Program, Travel Award
2019 Penn State Global Programs, Travel Award.
2017 NSF Rapid Grant OCE 1642311 (participation in project proposal).
2014 National Autonomous University of Mexico, Honorary Mention for MSc research